Double Negative Metamaterial Designs, Experiments, and Applications

Richard W. Ziolkowski

Electromagnetics Laboratory
Department of Electrical and Computer Engineering
University of Arizona
Tucson, Arizona 85721-0104

ziolkowski@ece.arizona.edu
Tel. (520) 621-6173
Fax. (520) 621-8076

Santa Barbara Center for Theoretical Physics
Quantum Optics Workshop: Week 1

Metamaterials

Artificial materials that exhibit electromagnetic responses generally not found in nature

Metamaterials exhibit qualitatively new response functions that are not observed in the constituent materials themselves and result, for instance, from the inclusion of artificially fabricated, extrinsic, low dimensional inhomogeneities

Examples:
- Artificial dielectrics
- FSS, Electromagnetic bandgap structures
- Negative index (neg eps, mu) materials

Metamaterials may lead to new physics and engineering concepts

Compact DNG metamaterials having negative index of refraction have been designed, fabricated and tested experimentally

- **HFSS and FDTD simulators have been used to design several DNG ($\varepsilon < 0$ and $\mu < 0$) metamaterials (MTMs)**
- **Extraction formula have been derived to determine the MTM's effective permittivity and permeability**
- **Experimental results confirm the realization of DNG MTMs that are matched to free space and have a negative index of refraction**
- **Several potential applications have been studied: Efficient Electrically Small Antennas (EESAs)**

Metamaterials lead to a variety of novel electromagnetic effects

- **The propagation characteristics of waves in DNG media ($\varepsilon < 0, \mu < 0$) confirm the possibility of a negative index of refraction**
- **Negative angles of refraction exist for DNG media**
- **DNG Drude MTMs have been characterized with an FDTD simulator and confirm**
  - **paraxial beam focusing**
  - **negative angles of refraction for power flow**
- **Demonstrate phase and phase front compensators**

EM Properties of aggregates of atoms / molecules are typically characterized by their electric and magnetic dipole moments

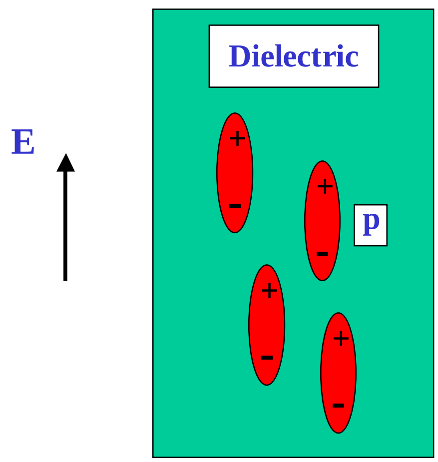

$P = \Sigma_i \, p_i / V$

$= \varepsilon_0 \, \chi \, E$

$\varepsilon = \varepsilon_0 \, (1 + \chi)$

χ = **electric susceptibility**

The Debye and Lorentz linear polarization models produce well-known material responses

Debye Model

$$\partial_t \, P_x + \Gamma_E \, P_x \, = \epsilon_0 \, \Gamma_E \, \chi_\alpha \, E_x$$

Lorentz Model

$$\partial_t^2 \, P_x + \Gamma_E \, \partial_t \, P_x + \omega_0^2 \, P_x \, = \, \epsilon_0 \, \omega_0^2 \, \chi_\alpha \, E_x$$

$$\hat{P}_x(\omega) = \frac{\omega_0^2 \, \chi_\alpha}{-\omega^2 + j\omega\Gamma_E + \omega_0^2} \;\; \epsilon_0 \, \hat{E}_x(\omega)$$

Drude Model

$$\partial_t^2 \, P_x + \Gamma_E \, \partial_t \, P_x \, = \, \epsilon_0 \, \omega_p^2 \, E_x$$

Several metamaterial models have been studied. They produce a variety of novel electromagnetic responses.

Time Derivative Debye Model

$$\partial_t P_x + \Gamma_E P_x = \epsilon_0 \Gamma_E \chi_\alpha E_x + \epsilon_0 \chi_\beta \partial_t E_x$$

Time-Derivative Lorentz Model

$$\partial_t^2 P_x + \Gamma_E \partial_t P_x + \omega_0^2 P_x = \epsilon_0 \omega_0^2 \chi_\alpha E_x + \epsilon_0 \omega_0 \chi_\beta \partial_t E_x$$

Two Time-Derivative Lorentz Model

$$\partial_t^2 P_x + \Gamma_E \partial_t P_x + \omega_0^2 P_x = \epsilon_0 \omega_0^2 \chi_\alpha E_x + \epsilon_0 \omega_0 \chi_\beta \partial_t E_x + \epsilon_0 \chi_\gamma \partial_t^2 E_x$$

These models have been implemented and tested with our 1D, 2D, and 3D FDTD simulators

Material responses are incorporated into our FDTD Maxwell equation solver through equivalent polarization and magnetization models

- ✯ Recursive Convolution Method

  $D = \varepsilon * E$

- ✢ Auxiliary Differential Equation Method

  $A(\partial_t)\, D = B(\partial_t)\, E$

- ✪ Polarization / Magnetization Method

  $A(\partial_t)\, P = B(\partial_t)\, E$

P & M equations are solved self-consistently with Maxwell equations

The matched DNG medium was simulated with a lossy Drude model

Lossy Drude permittivity

$$\epsilon(\omega) = \epsilon_0 \left(1 - \frac{\omega_{pe}^2}{\omega(\omega + i\Gamma_e)}\right)$$

Lossy Drude permeability

$$\mu(\omega) = \mu_0 \left(1 - \frac{\omega_{pm}^2}{\omega(\omega + i\Gamma_m)}\right)$$

Matching conditions

$$\omega_{pe} = \omega_{pm}$$
$$\Gamma_e = \Gamma_m$$
$$Z(\omega) = \sqrt{\frac{\mu(\omega)}{\epsilon(\omega)}} = \sqrt{\frac{\mu_0}{\epsilon_0}} = Z_0$$

The 1D time domain equations solved with the FDTD simulator for the matched DNG medium were straight-forward

$$\partial_t E_x = \frac{1}{\epsilon_0}\left(-\partial_z H_y - J_x\right)$$
$$\partial_t J_x + \Gamma J_x = \epsilon_0\, \omega_p^2\, E_x$$
$$\partial_t H_y = \frac{1}{\mu_0}\left(-\partial_z E_x - K_y\right)$$
$$\partial_t K_y + \Gamma K_y = \mu_0\, \omega_p^2\, H_y$$

Note: K_x has been normalized by μ_0 to make the magnetic current equation dual to the electric current definition.

Note: Matching is achieved by placing the E's, H's, J's and K's in FDTD cells in the correct manner

Real part of lossy Drude model for different plasma frequencies

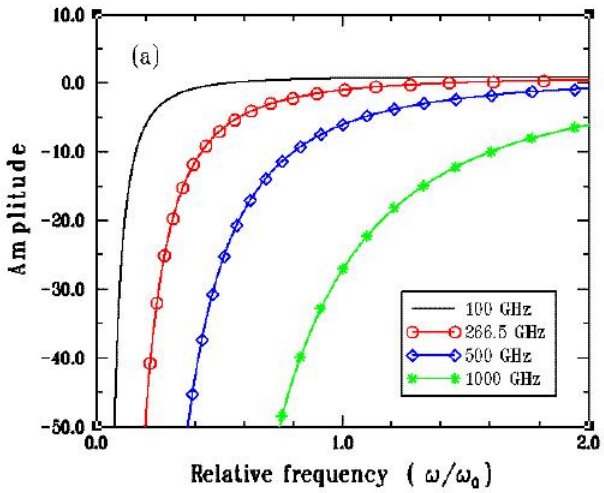

f_0 = 30 GHz

Wave properties in DNG media are "unusual"

- Wave propagation and power flow is causal
- The medium is right-handed with respect to the direction of propagation
- The medium is left-handed with respect to the direction the wave vector direction

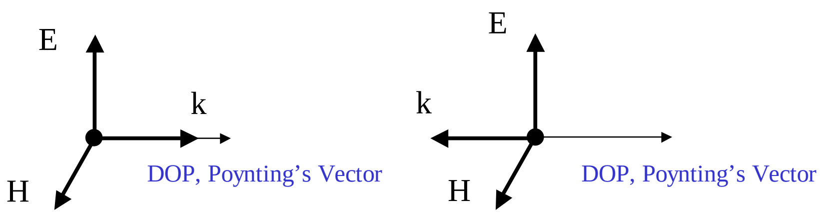

Normal

DNG

Ziolkowski and Heyman have determined the correct, causal square root choice and confirmed it with FDTD simulations

For a slightly lossy DNG medium

$$n \simeq -\sqrt{|\epsilon_r \mu_r|}\left[1 - i\,\frac{1}{2}\left(\frac{\epsilon_i}{|\epsilon_r|} + \frac{\mu_i}{|\mu_r|}\right)\right]$$

$$\zeta \simeq +\sqrt{|\mu_r/\epsilon_r|}\left[1 - i\,\frac{1}{2}\left(\frac{\mu_i}{|\mu_r|} - \frac{\epsilon_i}{|\epsilon_r|}\right)\right]$$

If $\epsilon < 0$ and $\mu < 0$,this means the correct causal choice gives

$$n_r(\omega) < 0 \qquad n_i(\omega) > 0$$

$$Z_r(\omega) > 0$$

Analytical and FDTD simulation problem geometries

Plane wave source

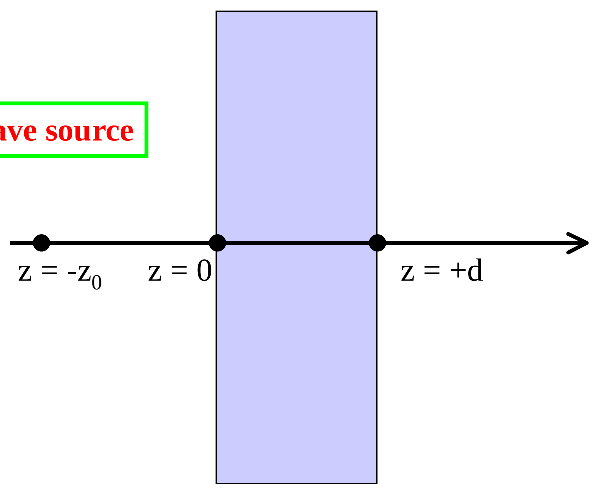

2TDLM slab, DNG slab

Response for Neg ε, Neg μ, and Matched DNG media

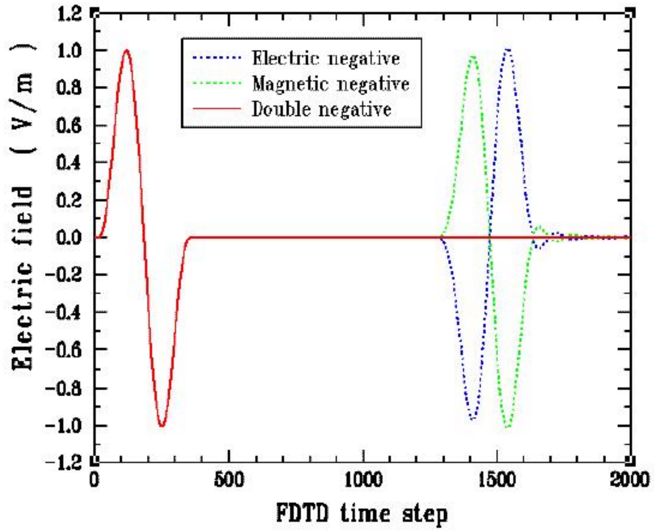

Several EM quantities were monitored

Correct form of Poynting's theorem in a dispersive medium

$$-\oint_{\Sigma=\partial V} \vec{S}\cdot\hat{n}_\Sigma\, d\Sigma = \int_V [\epsilon_0 \vec{E}\cdot\partial_t\vec{E} + \vec{E}\cdot\partial_t\vec{P} + \mu_0\vec{H}\cdot\partial_t\vec{H} + \mu_0\vec{H}\cdot\partial_t\vec{M}]\, dV$$

The form of Poynting's theorem in an homogenous, non-dispersive medium

$$-\oint_{\Sigma=\partial V} \vec{S}\cdot\hat{n}_\Sigma\, d\Sigma = \partial_t \int_V \left[\frac{1}{2}\epsilon|\vec{E}|^2 + \frac{1}{2}\mu|\vec{H}|^2\right] dV = \partial_t U_{EM}$$

The index of refraction

$$n_{FDTD} = \frac{1}{ik_0\,(z_2 - z_1)}\ \ln\left[\frac{\tilde{E}_x(z_2,\omega)}{\tilde{E}_x(z_1,\omega)}\right]$$

FDTD modeling of wave propagation in DNG media confirms causal behavior and negative index of refraction

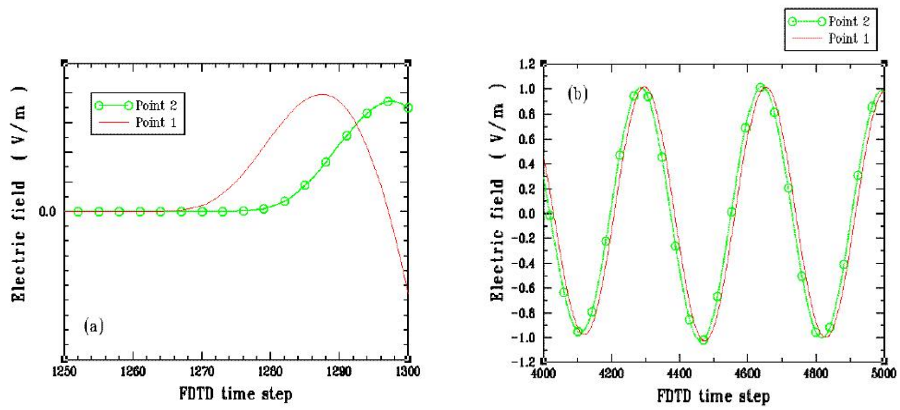

Early time **Late time**

The two time derivative Lorentz model produces a causal metamaterial response

Two Time-Derivative Lorentz Model

$$\partial_t^2 P_x + \Gamma_E \, \partial_t P_x + \omega_0^2 P_x = \epsilon_0 \, \omega_0^2 \, \chi_\alpha \, E_x + \epsilon_0 \, \omega_0 \, \chi_\beta \, \partial_t E_x + \epsilon_0 \, \chi_\gamma \, \partial_t^2 E_x$$

$$\hat{P}_x(\omega) = \frac{\omega_0^2 \, \chi_\alpha + j\omega \, \omega_0 \, \chi_\beta - \omega^2 \, \chi_\gamma}{-\omega^2 + j\omega\Gamma_E + \omega_0^2} \, \epsilon_0 \, \hat{E}_x(\omega)$$

This implies the limiting properties

$$\lim_{\omega \to 0} \frac{\epsilon(\omega)}{\epsilon_0} = 1 + \chi_\alpha$$

$$\lim_{\omega \to \infty} \frac{\epsilon(\omega)}{\epsilon_0} = 1 + \chi_\gamma$$

Susceptibility of 2TDLM material was designed to produce the desired superluminal medium response

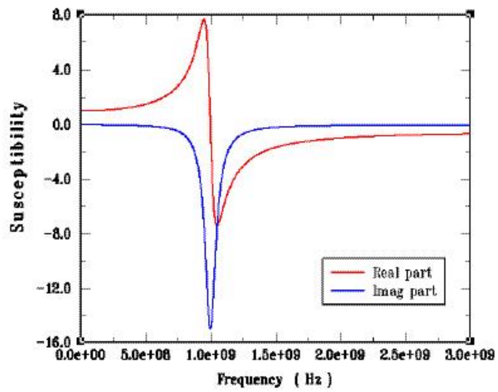

$\chi_\alpha = 1$, $\chi_\beta = 10^{-5}$, $\chi_\gamma = -0.5$, $\omega_p = \omega_0 = 1$ **GHz**

Propagation through 2TDLM slabs with χ_γ = +0.5, 0.0, -0.5 demonstrate the superluminal effect

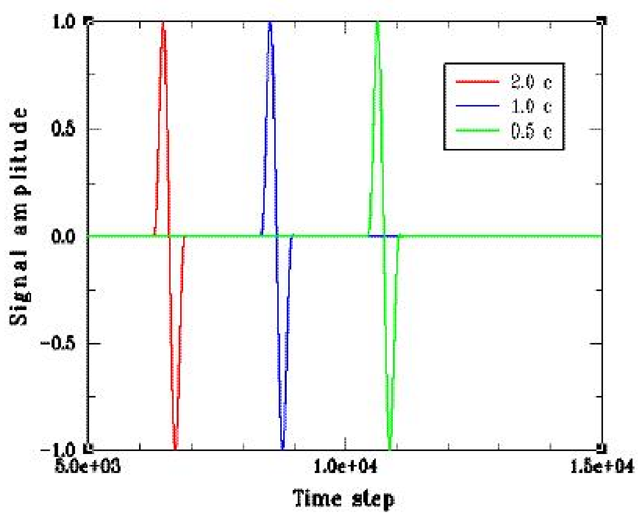

FDTD simulations of plane wave propagation through a matched 2TDLM metamaterial confirms the superluminal behavior

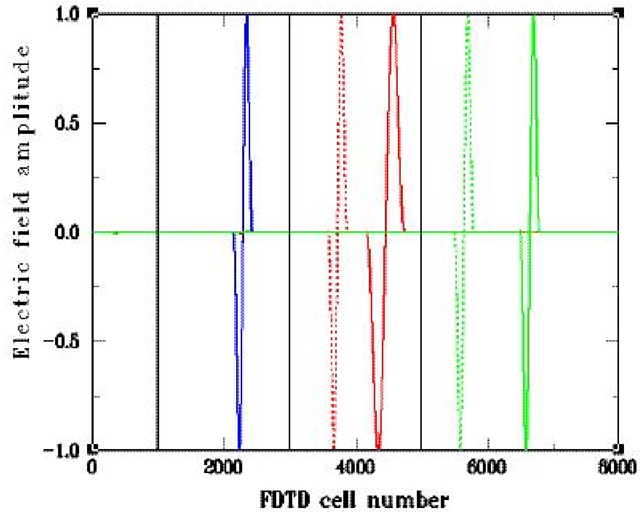

FDTD simulations of plane wave propagation through a matched 2TDLM metamaterial slab confirms the causal superluminal transmission of information

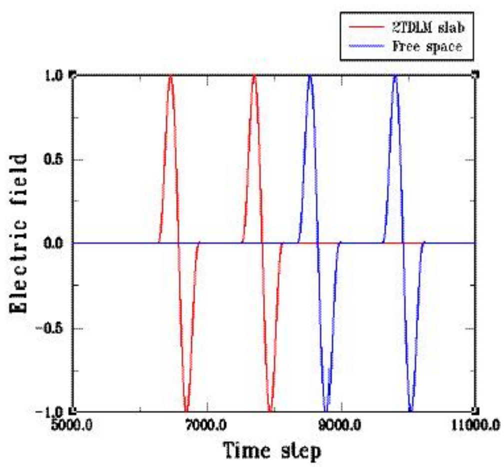

Double negative (DNG) media ($\epsilon < 0$ *and* $\mu < 0$) can be realized with metamaterial constructs

- "Perfect Lens Effect"
  Pendry, PRL Oct. 2000,
- Waves are not focused in general DNG medium but rather beams are produced
  Ziolkowski and Heyman, PRE, October 2001
- Direction of Power Flow
  Positive: Valanju, Walser, Valanju, PRL, May 2002
  Negative: Caloz, Xhang, Itoh, JAP, December 2001
  Negative: Kong, Wu, Zhang, Microwave Opt. Tech. Lett., April 2002
  Negative: Ziolkowski and Heyman, PRE, October 2001

General result: Beams are formed in the DNG slab rather than foci

NOTE: Slab solution is independent of square root choice

NOTE: Correct propagating and evanescent spectra

NOTE: Foci appear only for one special case:

$$\epsilon = -\epsilon_0,\ \mu = -\mu_0,\ n = -1$$

Then $\kappa = \kappa_0 = +1$ and a perfect foci appear for

$z_{f1} = |z_0|$ (in slab) $\quad z_{f2} = 2d - |z_0|$ (beyond slab)

General lossy, dispersive DNG slab: Beams are formed rather than foci

Paraxial result

$$g \approx \frac{1}{-2ik_0} e^{+ik_0(|z_0|-\tilde{n}z)} e^{-i\frac{k_t^2}{2k_0}(|z_0|-z/\tilde{n})} \qquad 0 < z < d$$

$$g \approx \frac{1}{-2ik_0} e^{+ik_0[z+|z_0|-d(1+\tilde{n})]} e^{-i\frac{k_t^2}{2k_0}[z+|z_0|-d(1+1/\tilde{n})]} \qquad z > d$$

If $z_{f1} < d$ and $z_{f2} > d$, Paraxial foci appear at

$$z_{f1} = \tilde{n}|z_0|, \qquad z_{f2} = d(1 + 1/\tilde{n}) - |z_0|$$

Note: $z_{f1} = d/2$ if $z_0 = d/2\tilde{n}$ and $z_{f2} = d(1 + 1/2\tilde{n})$

Analytical and FDTD simulation problem geometries

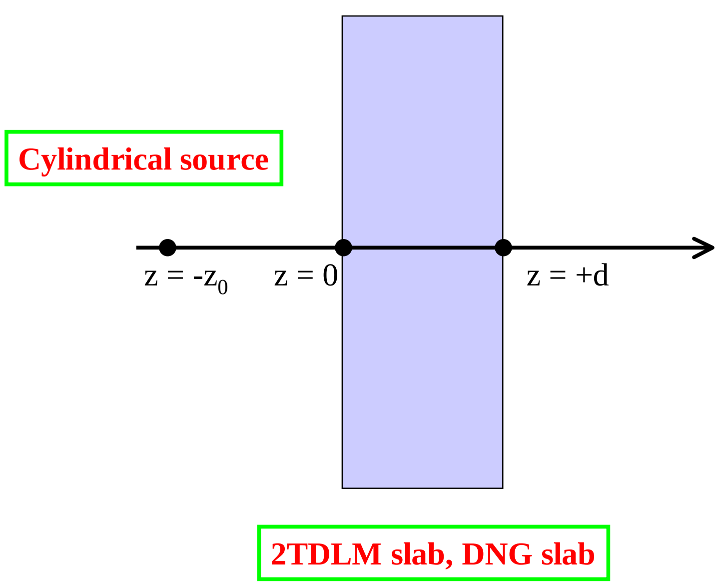

FDTD simulations of cylindrical wave interaction with lossy Drude DNG slab with $\varepsilon(\omega_0)/\varepsilon_0 = \mu(\omega_0)/\mu_0 = -1$ show no foci

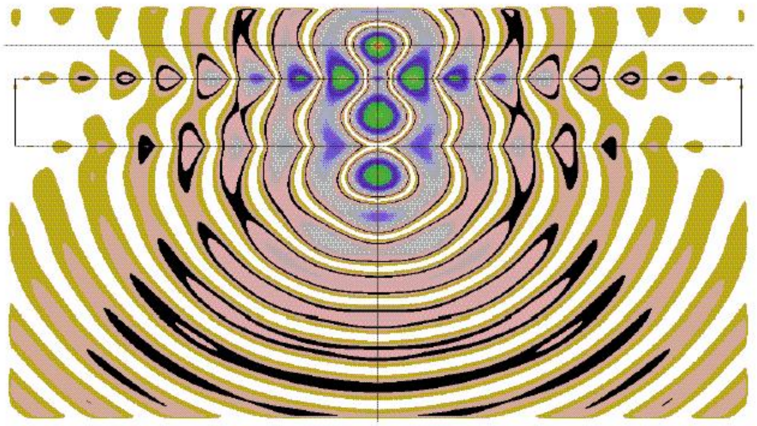

Electric field intensity at one time over FDTD simulation space

FDTD simulations of cylindrical wave interaction with lossy Drude DNG slab with $\varepsilon(\omega_0)/\varepsilon_0 = \mu(\omega_0)/\mu_0 = -6$ show the predicted beam formation

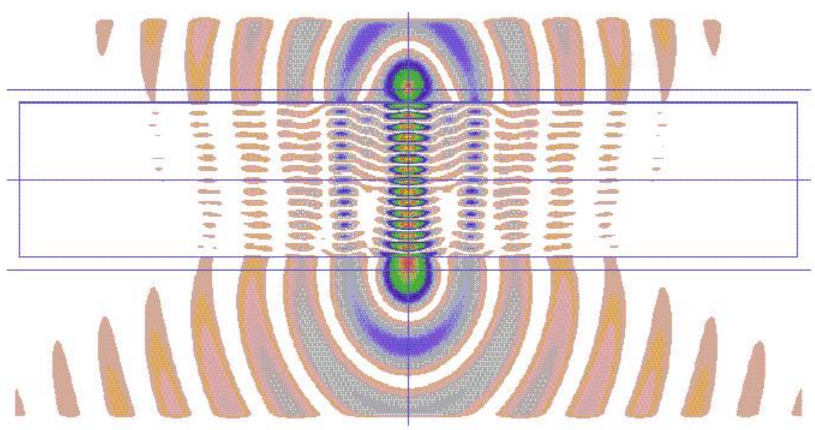

Electric field intensity at one time over FDTD simulation space

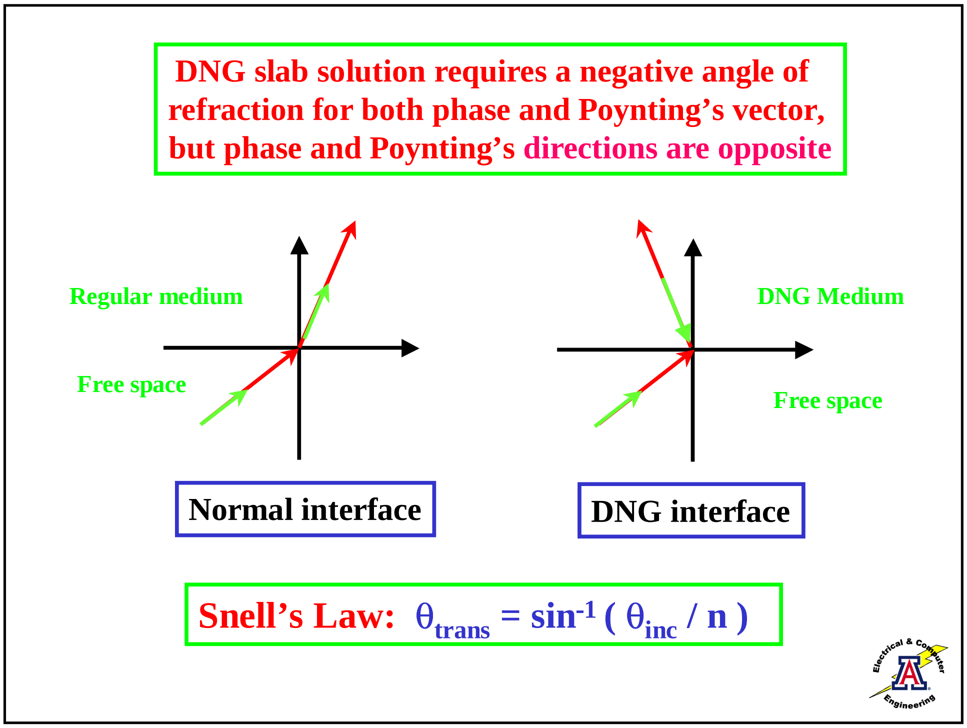
DNG slab solution requires a negative angle of refraction for both phase and Poynting's vector, but phase and Poynting's directions are opposite
Regular medium
Free space
DNG Medium
Free space
Normal interface
DNG interface
Snell's Law: $\theta_{trans} = \sin^{-1} (\theta_{inc} / n)$
Electrical & Computer Engineering

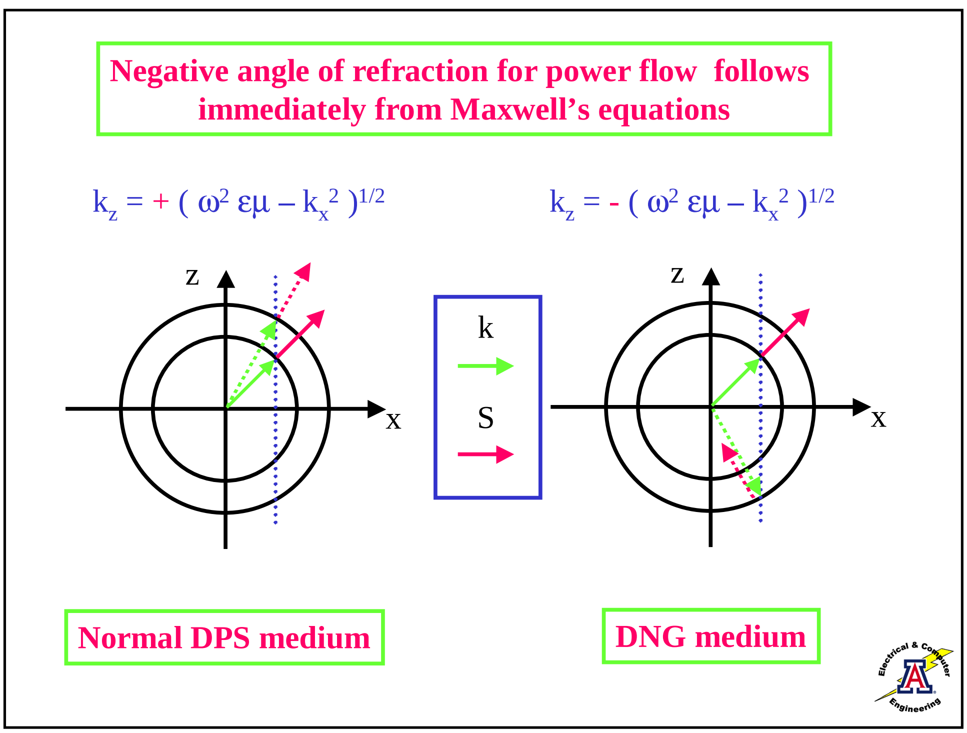
Negative angle of refraction for power flow follows immediately from Maxwell's equations
$k_z = + (\omega^2 \varepsilon\mu - k_x^{2})^{1/2}$
$k_z = - (\omega^2 \varepsilon\mu - k_x^{2})^{1/2}$
z
x
k
S
z
x
Normal DPS medium
DNG medium
Electrical & Computer Engineering

Super-prism effect requires local modifications of the wave vector – index surface

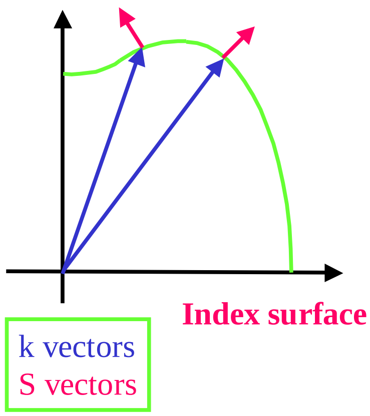

- EBG produces local curvature variations in the index surface
- Poynting’s vector is perpendicular to index surface
- Negative angle of refraction is realized
- Are the CLS-CLL metamaterial effects the same??
- Material extraction indicates simpler DNG properties

• Superprism effect (negative index of refraction) associated with EBGs (electromagnetic bandgaps) Notomi, Kosaka, …

Electric field intensity at one time over FDTD simulation space

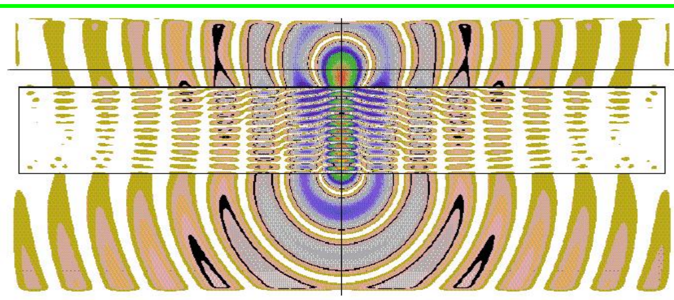

Poynting’s vector amplitude at one time over FDTD simulation space

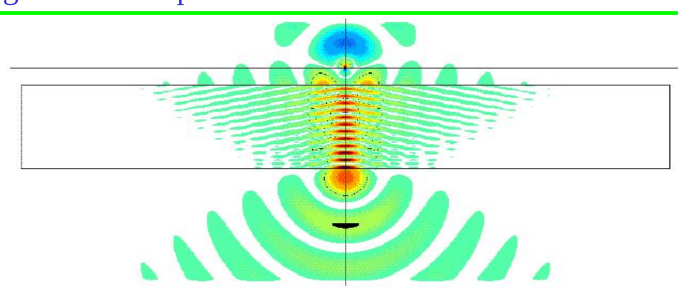

Source Plane →

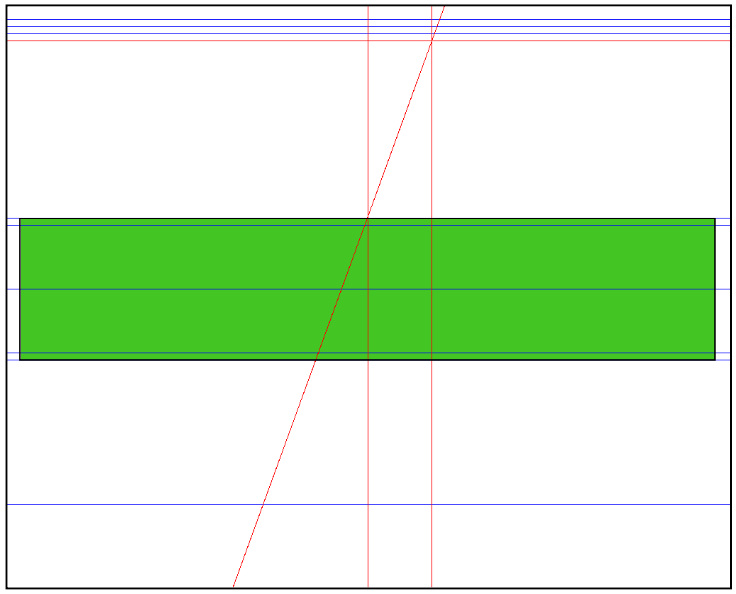

Geometry of larger FDTD problem that models a finite ($w_0=\lambda$) Gaussian beam interacting with a n = -1 DNG Drude MTM Slab

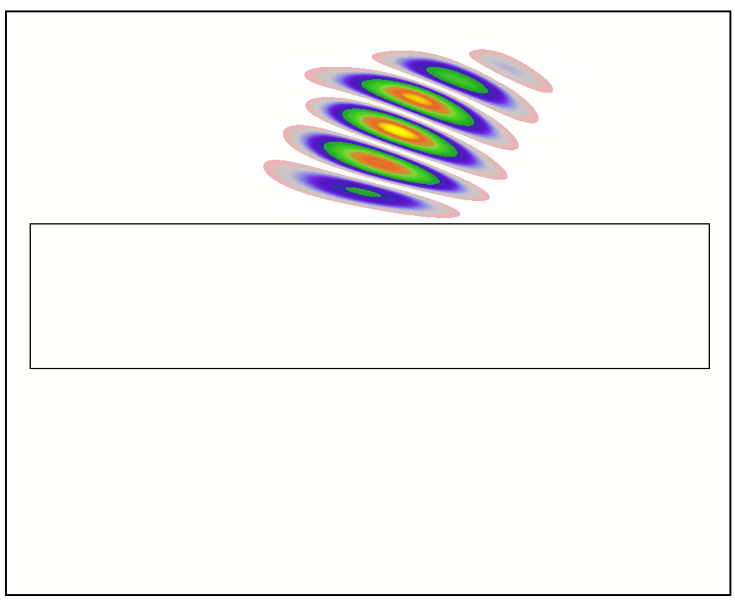

Electric Field Intensity

Early in time for a 20 degree angle of incidence, 3-cycle Gaussian beam interacting with a n = -1 at 30 GHz, Low Loss DNG slab

Electric
Field
Intensity

At a time
when a 20
degree
angle of
incidence
3-cycle
Gaussian
beam
is
interacting
with a
n = -1 at
30 GHz,
Low Loss
DNG slab

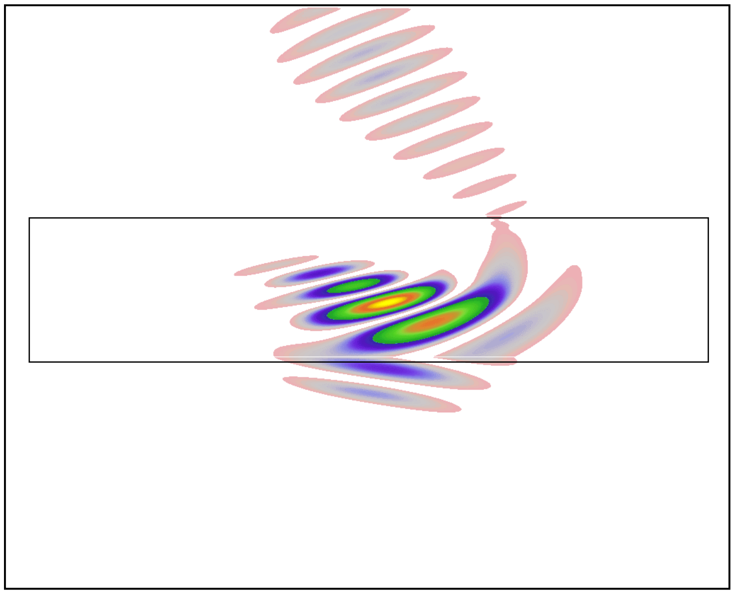

Electric
Field
Intensity

At a time
when a 20
degree
angle of
Incidence,
3-cycle
Gaussian
beam
has finished
interacting
with a
n = -1 at
30 GHz,
Low Loss
DNG slab

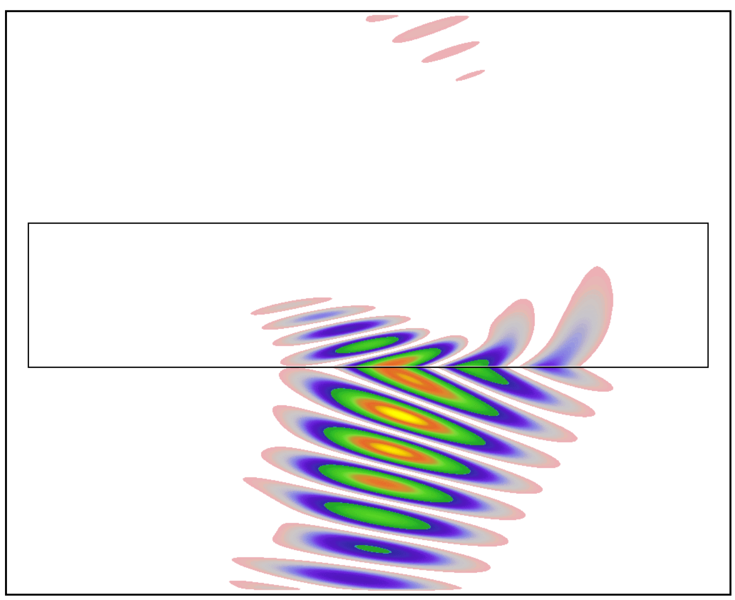

Electric Field Intensity

Late in time for a 20 degree angle of incidence, CW Gaussian beam interacting with a n = -1 at 30 GHz, Low Loss DNG slab

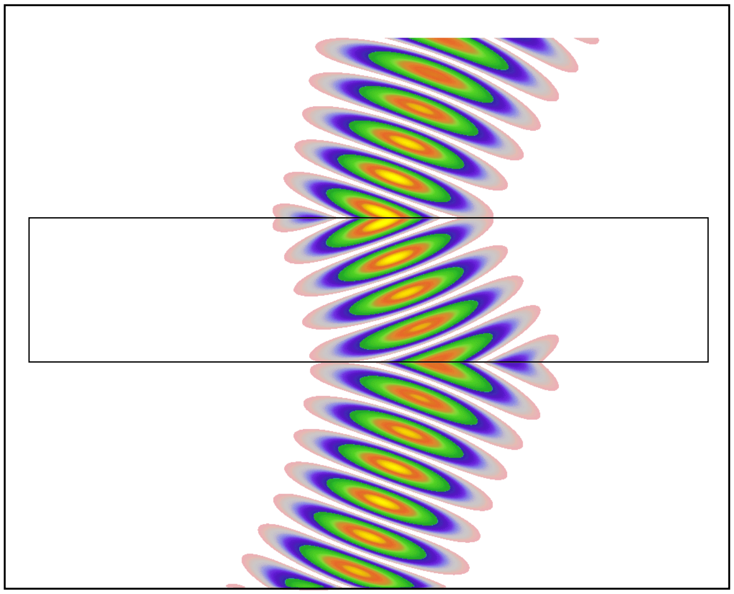

Source → Plane

Geometry of smaller FDTD problem that models a finite ($w_0=\lambda$) Gaussian beam interacting with a n = -6 DNG Drude MTM Slab

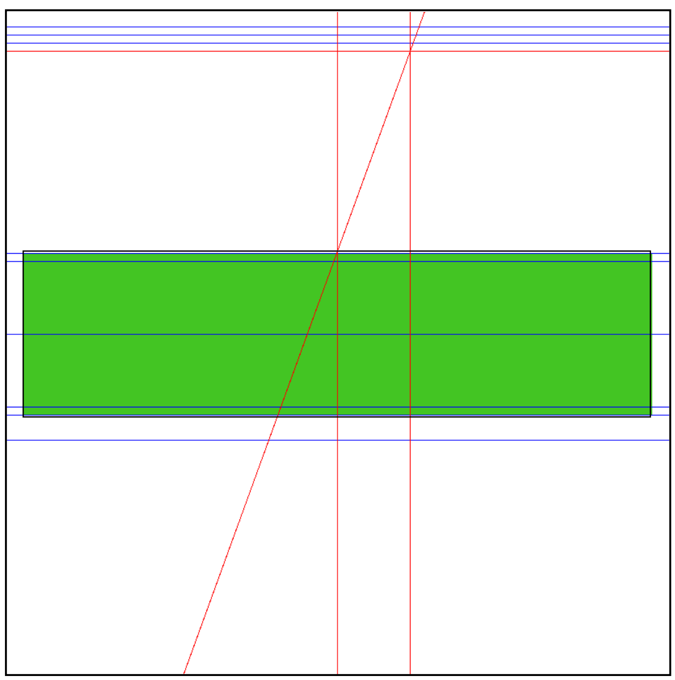

Electric
Field
Intensity

Early in
time
for a
20 degree
angle of
incidence,
3-cycle
Gaussian
beam
interacting
with a
n = -6 at
30 GHz,
Low Loss
DNG slab

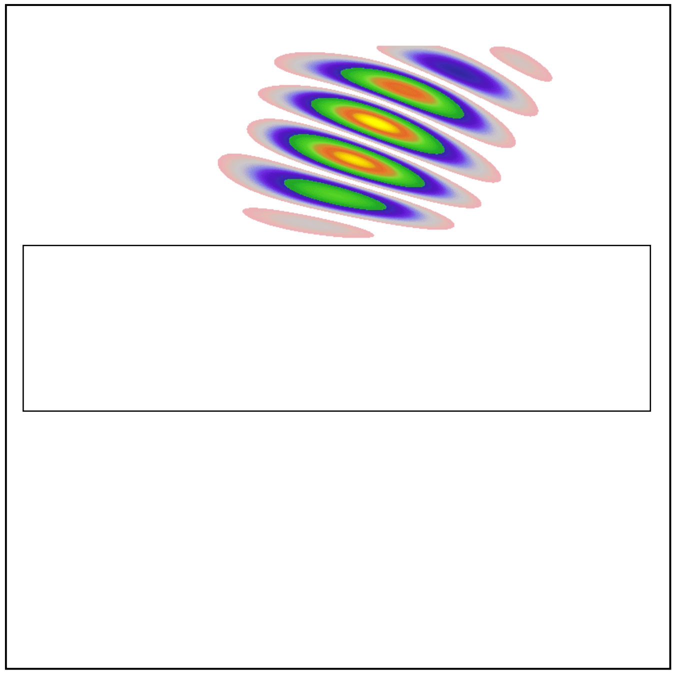

Electric
Field
Intensity

At a time
when a 20
degree
angle of
incidence
3-cycle
Gaussian
beam
is
interacting
with a
n = -6 at
30 GHz,
Low Loss
DNG slab

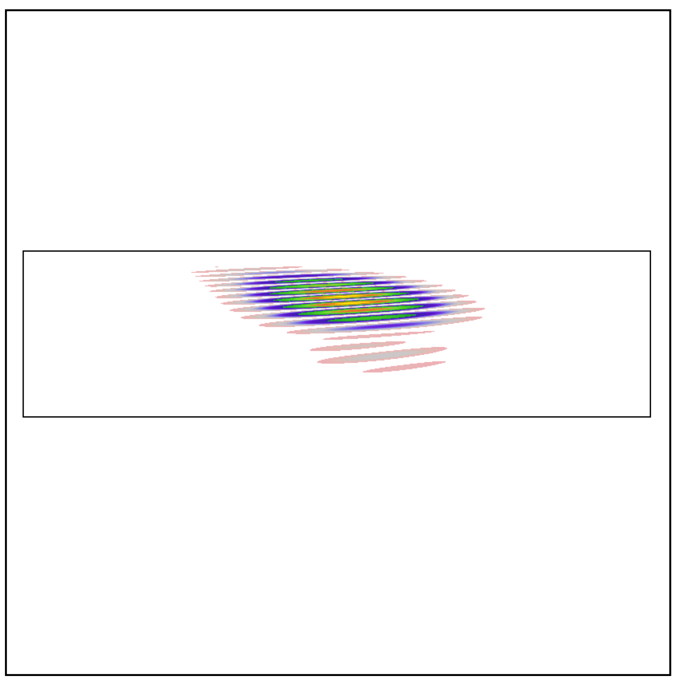

Electric Field Intensity

At a slightly later time when a 20 degree angle of incidence 3-cycle Gaussian beam is still interacting with a n = -6 at 30 GHz, Low Loss DNG slab

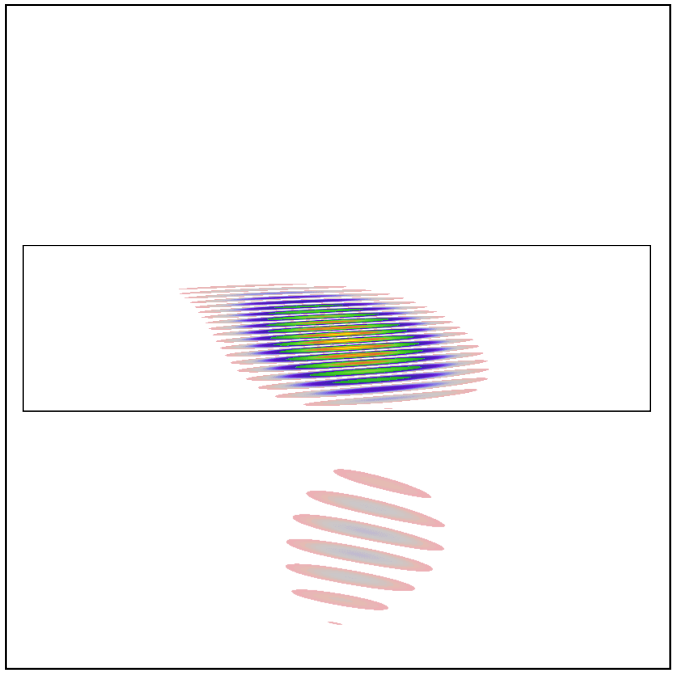

Electric Field Intensity

At a time when a 20 degree angle of Incidence, 3-cycle Gaussian beam has finished interacting with a n = -6 at 30 GHz, Low Loss DNG slab

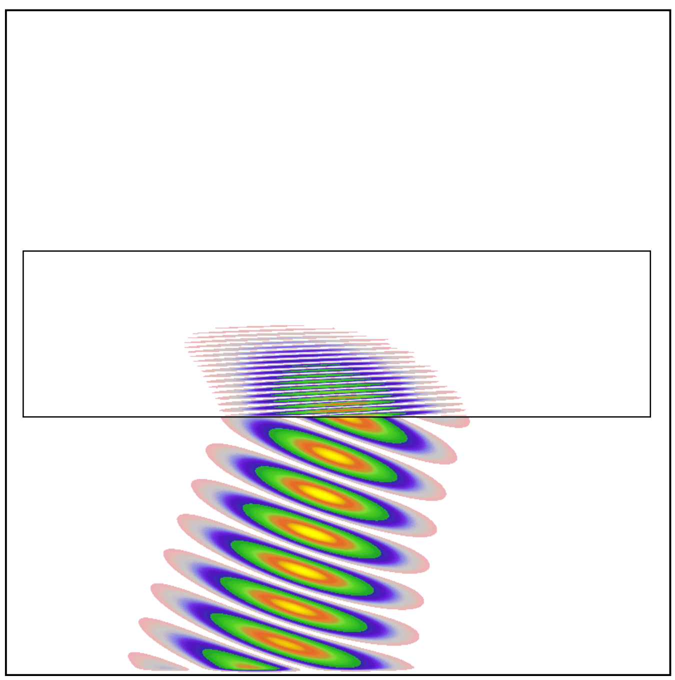

Electric Field Intensity

Late in time for a 20 degree angle of incidence, CW Gaussian beam interacting with a n = -6 at 30 GHz, Low Loss DNG slab

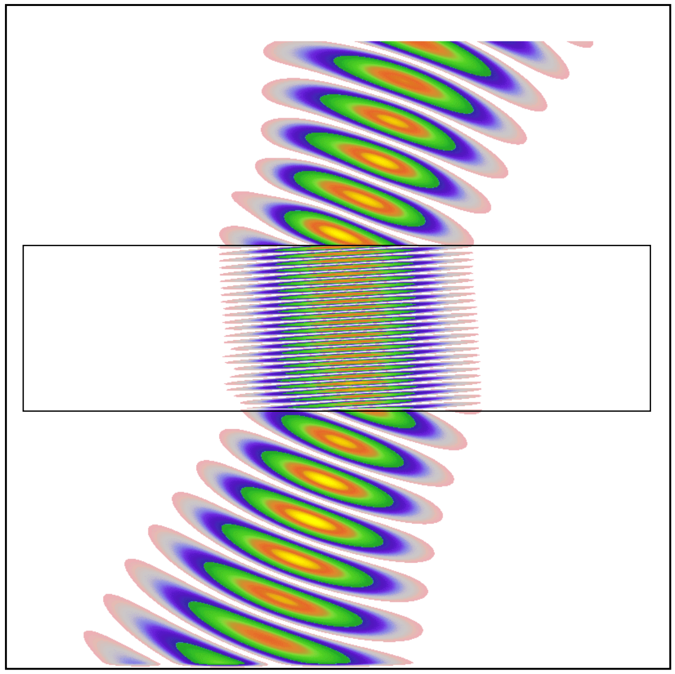

A DNG slab channels the electromagnetic field energy into a paraxial beam

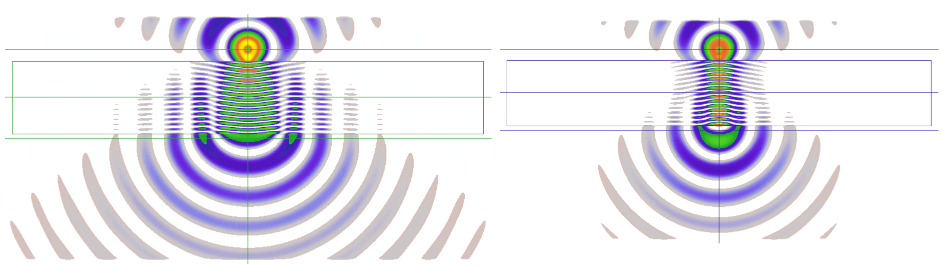

DPS Slab **DNG Slab**

Distribution of $|E|^2$ at the same time for a CW source

Matched DNG medium could lead to phase compensation techniques and devices

Matched media: **$Z = Z_0$ so there are no reflections**

$$R = (Z - Z_0) / (Z + Z_0) = 0$$

Negative Phase: **A DNG slab combined with a device that produces a positive phase shift, could lead to a zero phase point at the output of the combined device-slab**

DNG slabs can be used to achieve phase front compensation

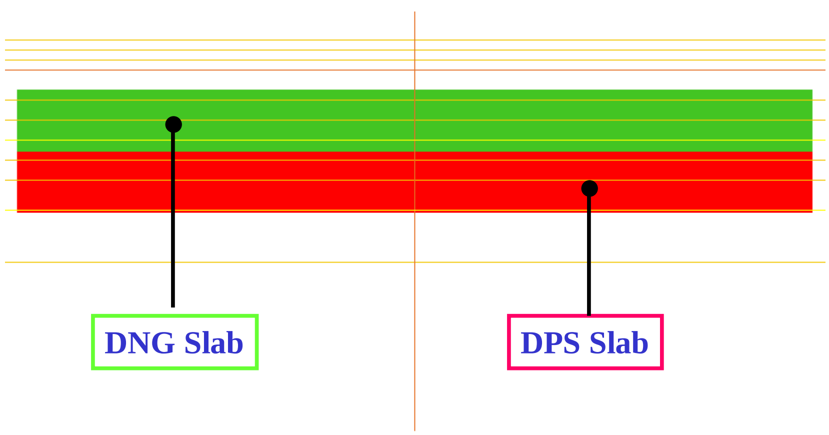

The phase fronts converge in the DNG slab

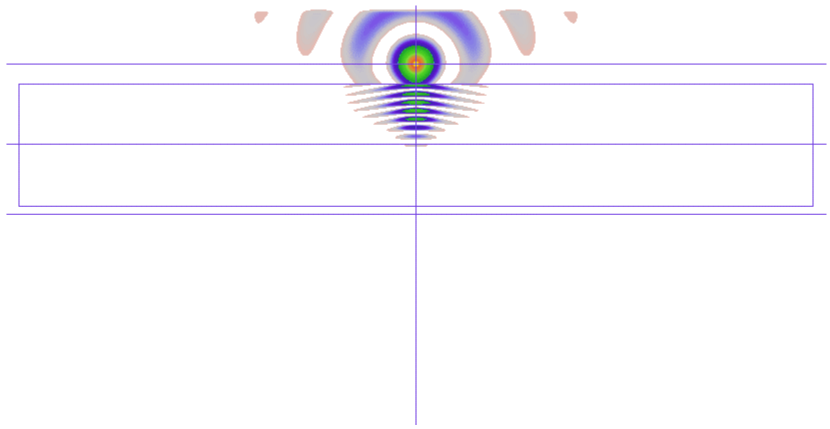

Distribution of $|E|^2$ at a single time instant early in the FDTD simulation

The phase fronts diverge in the DPS slab

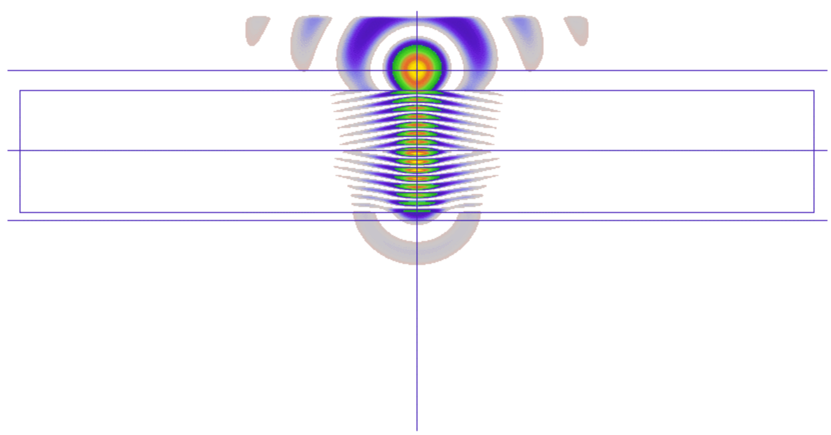

Distribution of $|E|^2$ at a single time instant

The phase fronts are planar near their exit from the DNG-DPS slab combination => 0° phase-shift delay line

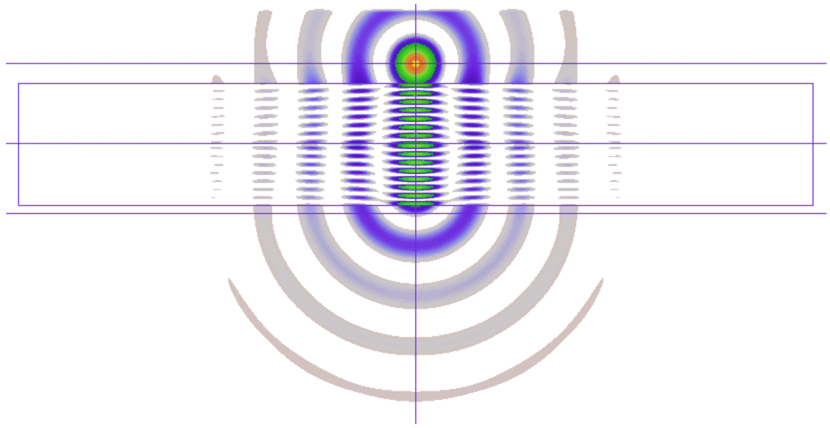

Distribution of $|E|^2$ at a single time instant
fter steady state is achieved

Compact metamaterials having negative index of refraction have been designed, fabricated and tested experimentally

- All structures constructed with Rogers Corporation
  5880 Duroid ($\varepsilon_r = 2.2$, $\mu_r = 1.0$, tan d = 0.0009)
  31 mil (100 mil = 2.54 mm) thick,
  125 mil polyethylene spacers
- S-parameters measured with a free space measurement
  system at X-band frequencies
- Experimental results confirm the realization of DNG MTMs
  that are matched to free space
- Very good agreement between numerical and
  experimental results

Electric dipole metamaterial

5 layers

31 x 24 elements

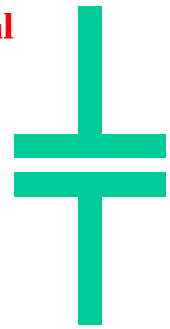

Unit element

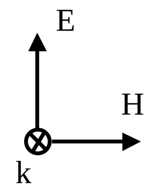

Magnetic dipole metamaterial

34 x 4 elements

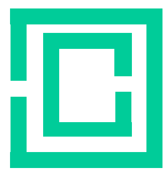

Unit element

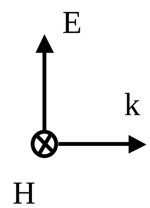

The first experiments only measured the orthogonal structure's components separately

Dipoles Only

Split rings only

Second series of measurements were performed to confirm the HFSS simulation results showing the DNG medium effects for the planar structure

CLSs, SRRs, & composite planar structure

Free space measurement system

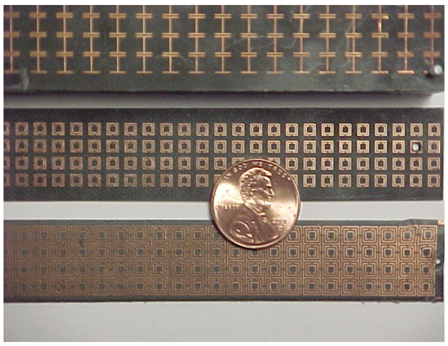

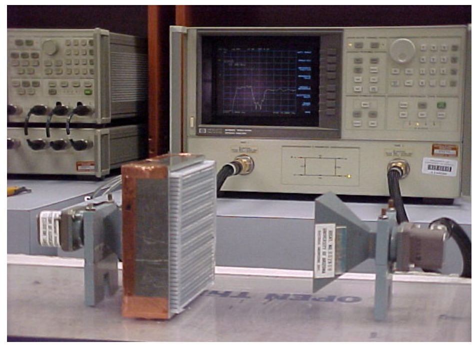

The S_{21} experimental data shows the predicted reflection bands for the electric and magnetic dipole metamaterials

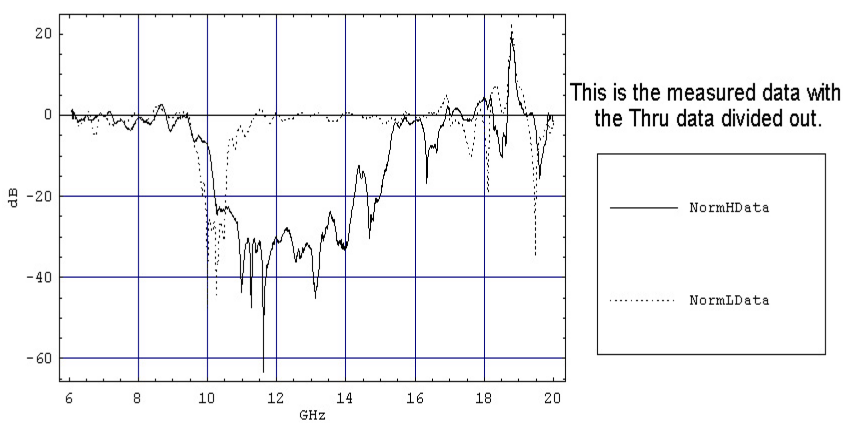

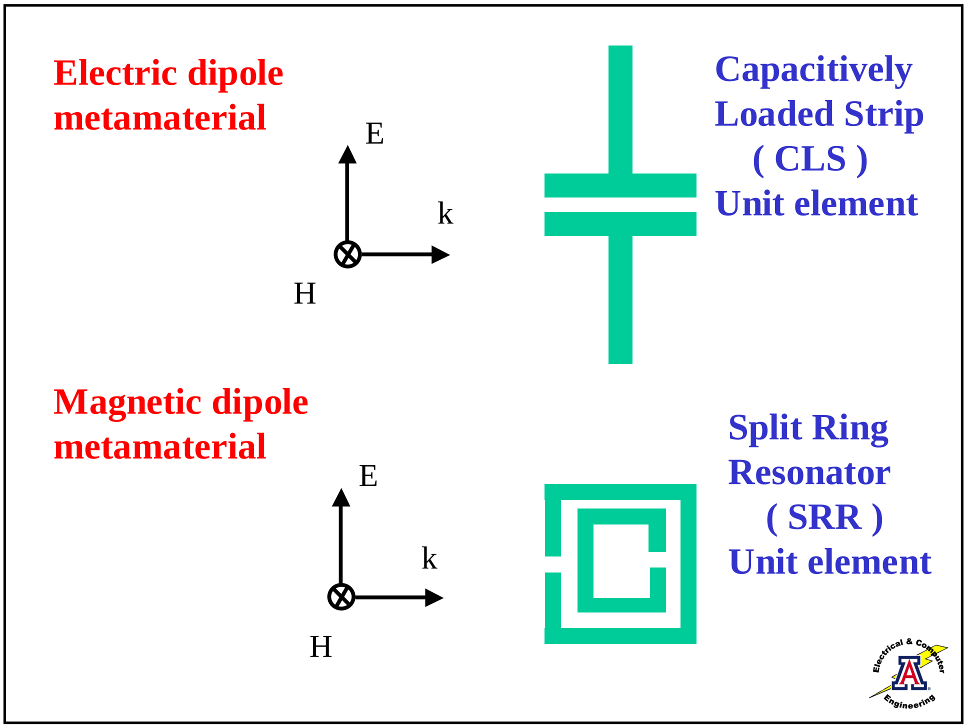
Electric dipole metamaterial
E
k
H
Capacitively Loaded Strip (CLS) Unit element
Magnetic dipole metamaterial
E
k
H
Split Ring Resonator (SRR) Unit element

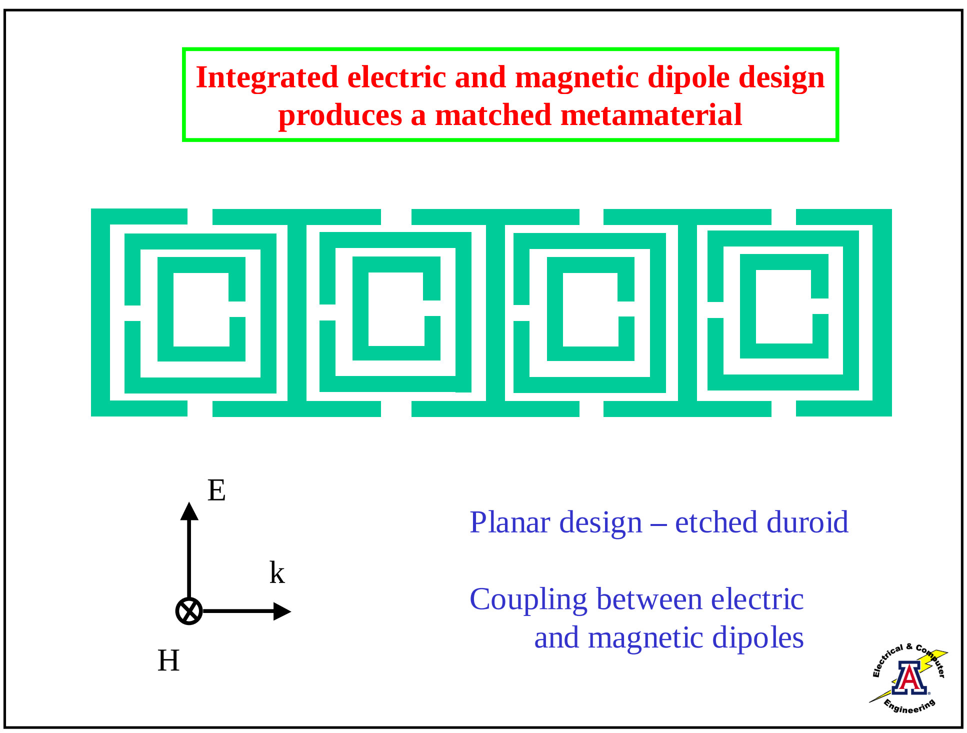
Integrated electric and magnetic dipole design produces a matched metamaterial
E
k
H
Planar design – etched duroid
Coupling between electric and magnetic dipoles

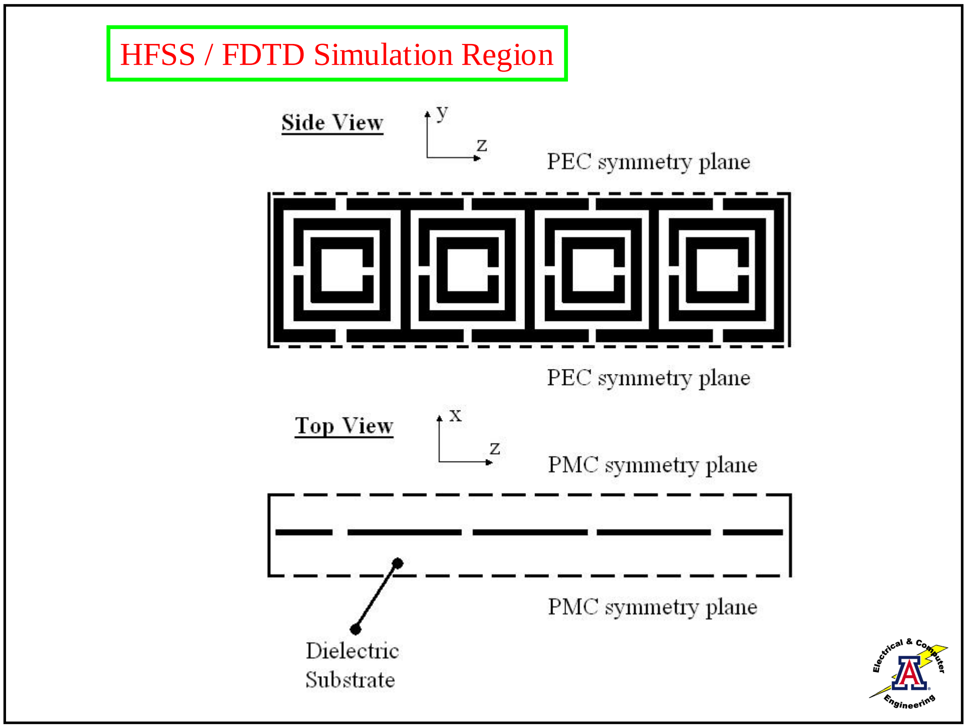
HFSS / FDTD Simulation Region
Side View
y
z
PEC symmetry plane
PEC symmetry plane
Top View
x
z
PMC symmetry plane
PMC symmetry plane
Dielectric
Substrate

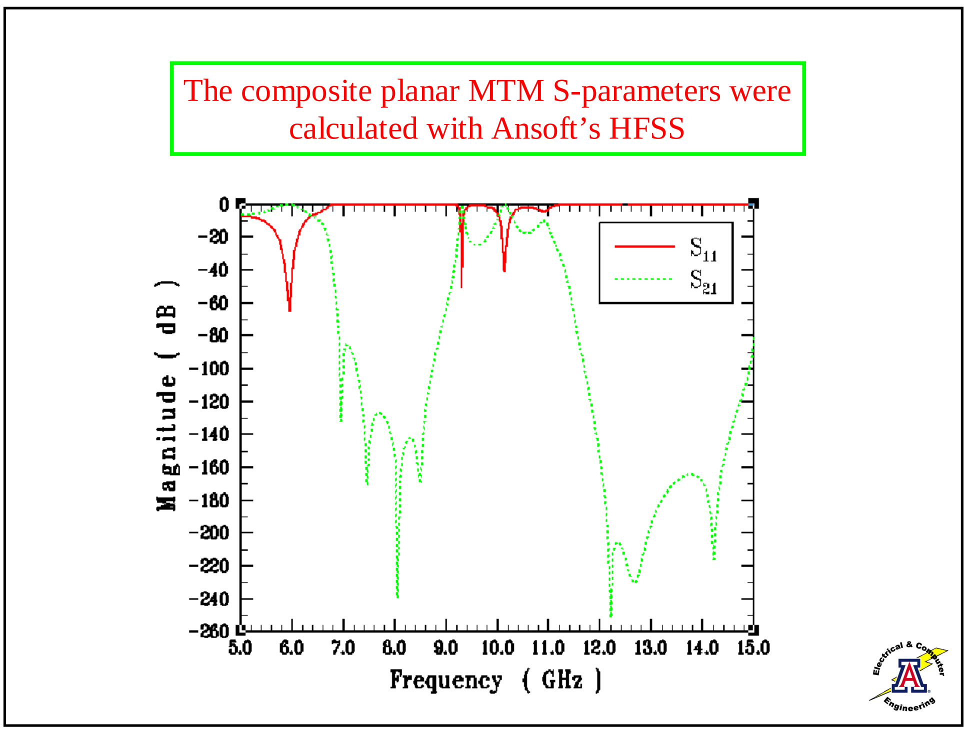
The composite planar MTM S-parameters were calculated with Ansoft's HFSS
Magnitude (dB)
0
-20
-40
-60
-80
-100
-120
-140
-160
-180
-200
-220
-240
-260
5.0
6.0
7.0
8.0
9.0
10.0
11.0
12.0
13.0
14.0
15.0
Frequency (GHz)
S11
S21

The effective permittivity and permeability were extracted from the HFSS S-parameter calculations

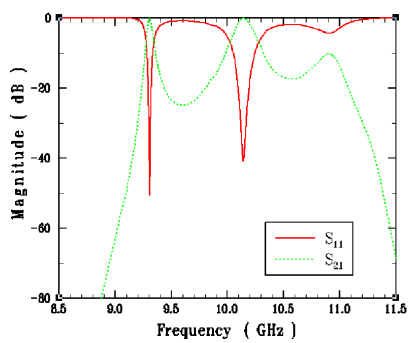

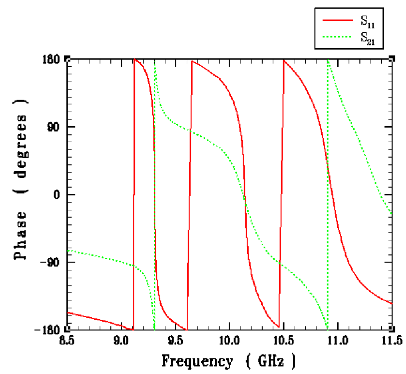

The composite planar MTM exhibits matching to free space in two frequency regions (and nearly three)

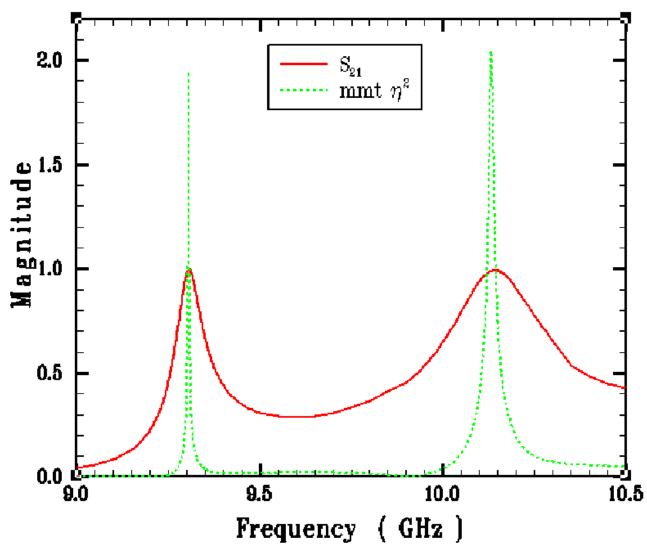

The S_{21} experimental data shows the predicted broad transmission band for the matched DNG medium

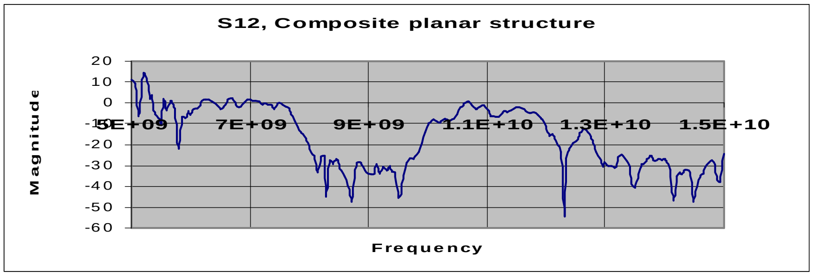

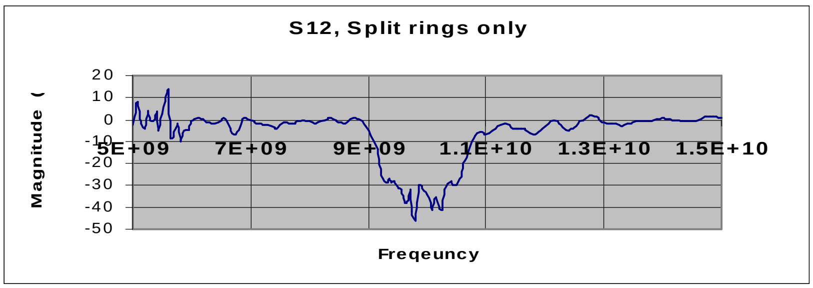

Effective permittivity and permeability parameters are commonly extracted from S-parameter (calculated/measured) values using the Nicolson, Ross, and Weir approach

$$V_1 = S_{21} + S_{11}$$
$$V_2 = S_{21} - S_{11}$$

$$X = \frac{1 + V_1 V_2}{V_1 + V_2}$$
$$Y = \frac{1 - V_1 V_2}{V_1 - V_2}$$

$$Z = \exp(ikd) = X \pm \sqrt{X^2 - 1}$$
$$\Gamma = Y \pm \sqrt{Y^2 - 1}$$

$$k_0 = \frac{\omega}{c}$$

$$\sqrt{\varepsilon_r \mu_r} = \frac{\ln(Z)}{jk_0 d}$$

$$\sqrt{\frac{\mu_r}{\varepsilon_r}} = \frac{1+\Gamma}{1-\Gamma}$$

$$\mu_r = \frac{1+\Gamma}{1-\Gamma}\frac{\ln(Z)}{jk_0 d}$$

$$\varepsilon_r = \frac{1-\Gamma}{1+\Gamma}\frac{\ln(Z)}{jk_0 d}$$

The effective permittivity and permeability parameters were extracted from the S-parameter values using a modified version of the Nicolson, Ross, and Weir approach

$$\exp(ikd) = \frac{V_1 - \Gamma}{1 - \Gamma V_1}$$

$$\Gamma = \frac{\exp(ikd) - V_2}{1 - V_2 \exp(ikd)}$$

$$1 - \exp(ikd) = \frac{(1-V_1)(1+\Gamma)}{1 - \Gamma V_1}$$

$$\sqrt{\frac{\mu_r}{\varepsilon_r}} = \frac{1-\exp(ikd)}{1+\exp(ikd)} \frac{1-V_2}{1+V_2}$$

$$\sqrt{\varepsilon_r \mu_r} \approx \frac{1}{jk_0 d} \frac{(1-V_1)(1+\Gamma)}{1-\Gamma V_1}$$

$$\mu_r \approx \frac{2}{jk_0 d} \frac{1-V_2}{1+V_2}$$

$$\varepsilon_r \approx \left(\frac{k}{k_0}\right)^2 \frac{1}{\mu_r}$$

$$n = \sqrt{\varepsilon_r}\sqrt{\mu_r}$$

$$\varepsilon_r \approx \mu_r - \frac{2}{jk_0 d} S_{11}$$

Enhanced result when $S_{11} \sim 0$

A simplified MTM was designed to isolate the electric and magnetic elements and the corresponding effects

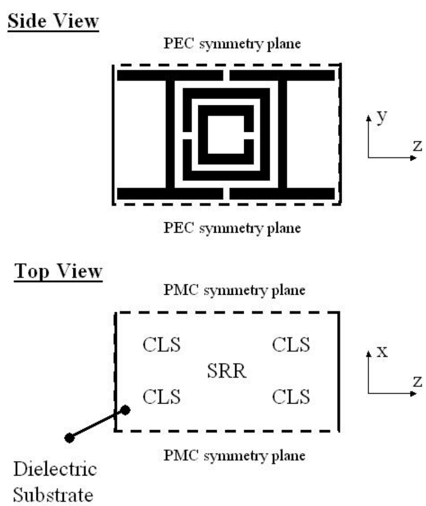

CLS-only MTM

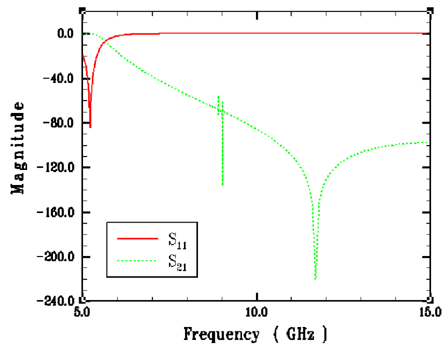

S-parameters, Ansoft's HFSS

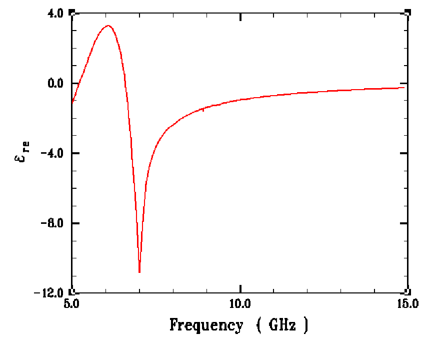

Extracted effective permittivity

SRR-only MTM

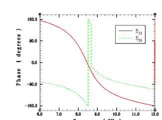

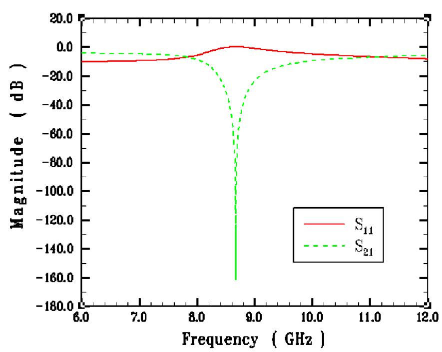

S-parameters, Ansoft's HFSS

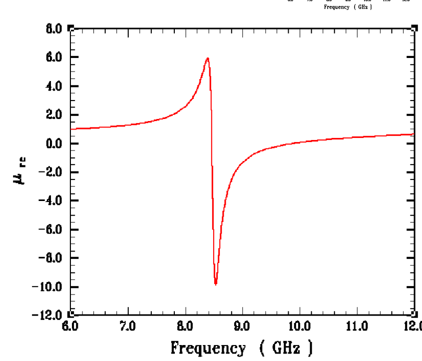

Extracted effective permeability

The effective material responses raise interesting issues

$$\chi_e = \frac{\omega_p^2 \chi_L}{-\omega^2 + j\Gamma\omega + \omega_0^2} \Rightarrow \varepsilon_r \approx 1 - \frac{\omega_p^2 \chi_L}{\omega^2 - \omega_0^2}$$

Lorentz Model

$$\varepsilon_r \approx 1 - \frac{\omega_p^2}{\omega^2}$$

Drude Model

$$\chi_m = \frac{-\chi_\gamma \omega^2 + j\chi_\beta \omega_p \omega + \chi_\alpha \omega_p^2}{-\omega^2 + j\Gamma\omega + \omega_0^2} \Rightarrow \mu_r \approx 1 - \frac{|\chi_L|\,\omega^2}{\omega^2 - \omega_0^2}$$

Two Time Derivative Lorentz Model

Composite MTM structure

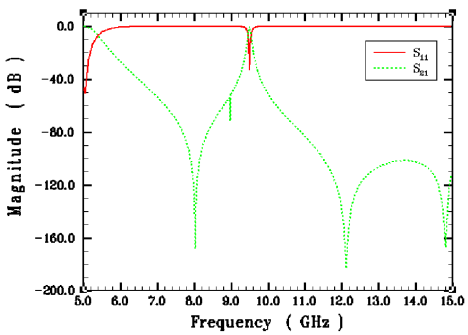

S-parameters, Ansoft's HFSS

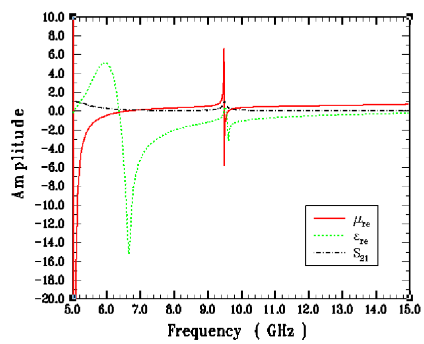

Extracted effective permittivity and permeability

The effective index of refraction of the simplified MTM is negative in the frequency region were matching occurs

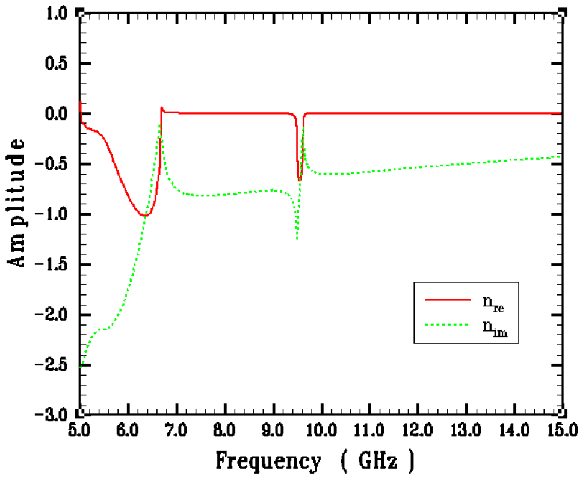

The effective permittivity and permeability of the composite planar MTM were extracted from the HFSS S-parameter calculations

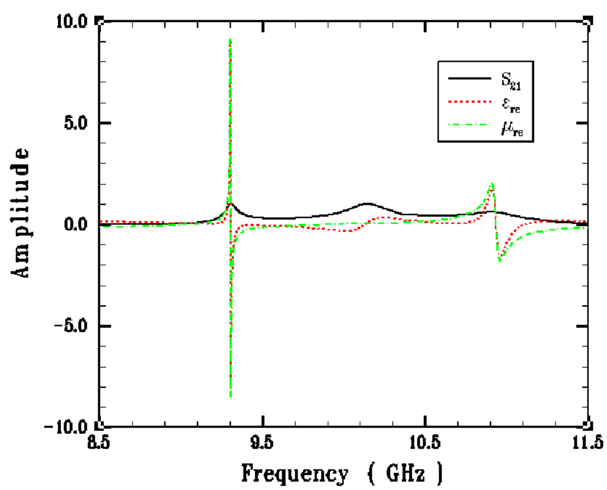

A negative effective index of refraction was extracted from the HFSS S-parameter calculations and from the FDTD calculations

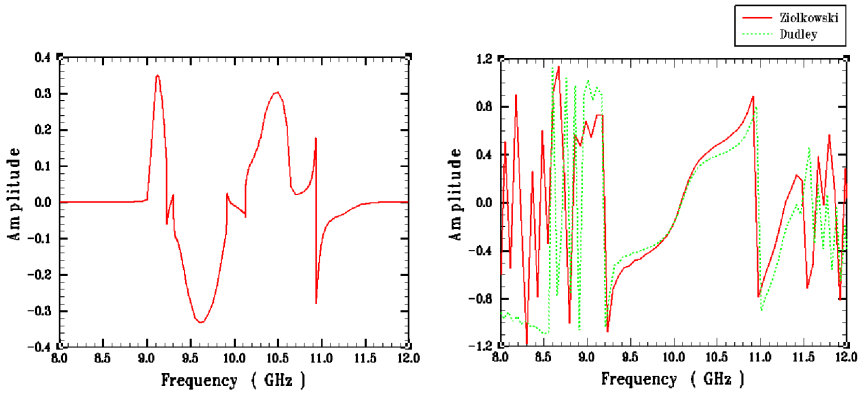

HFSS results

FDTD results

Confirmation that negative index of refraction MTMs have been realized

Metamaterials and improved antenna performance: Artificial perfect magnetic conductors (PMCs) – High Z surfaces

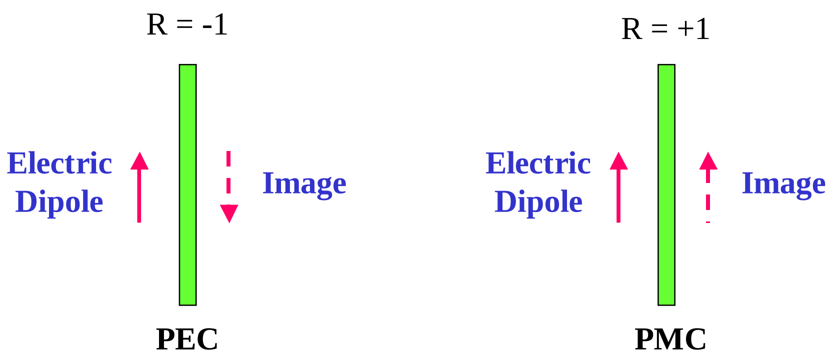

- Double the field strength
- Increase the bandwidth (Hansen)

SRR Design with Dimensions

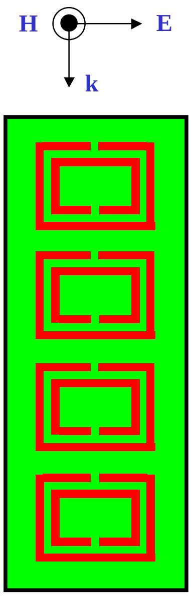

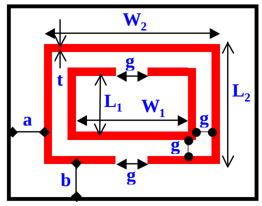

One element unit cell

g	10 mils
t	10 mils
L_1	55 mils
W_1	55 mils
L_2	95 mils
W_2	95 mils
a	25 mils
b	20 mils

100 mils = 2.54 mm

HFSS calculated S_{11} values for the SRR MTM with a depth of 1, 2, 3, 4 SRR elements show complete reflectivity near the design frequency of 10GHz

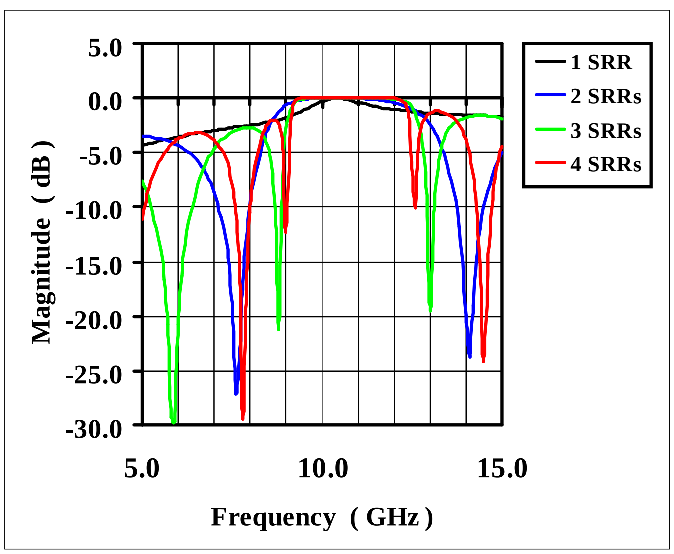

HFSS calculated S_{11} values for the SRR MTM with a depth of 4 SRR elements show that it acts as a PMC near the design frequency of 10GHz

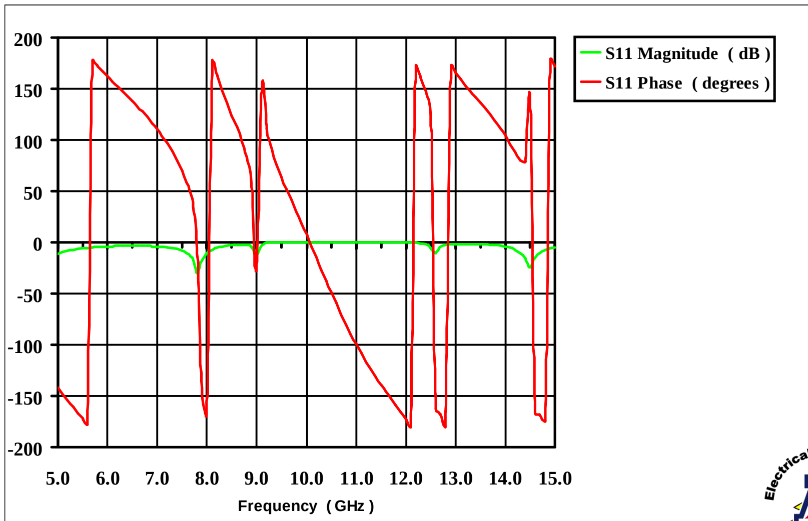

CLL Design with Dimensions

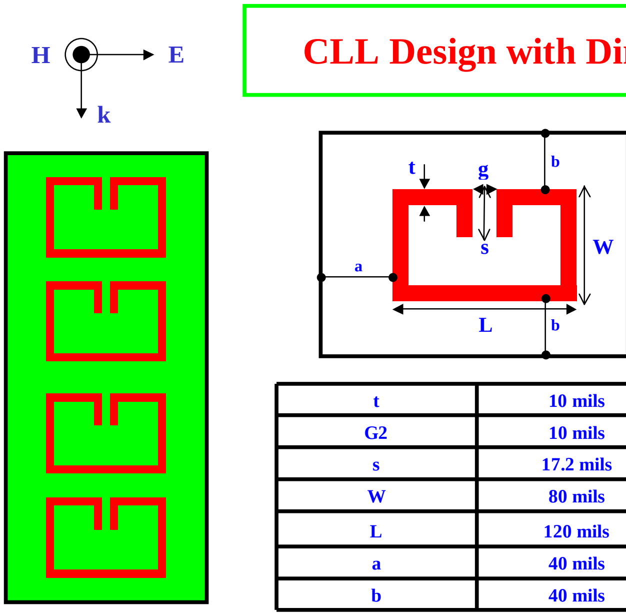

One element unit cell

t	10 mils
G2	10 mils
s	17.2 mils
W	80 mils
L	120 mils
a	40 mils
b	40 mils

100 mils = 2.54 mm

HFSS calculated S_{11} values for the SRR MTM with a depth of 1, 2, 3, 4 CLL elements show complete reflectivity near the design frequency of 10GHz

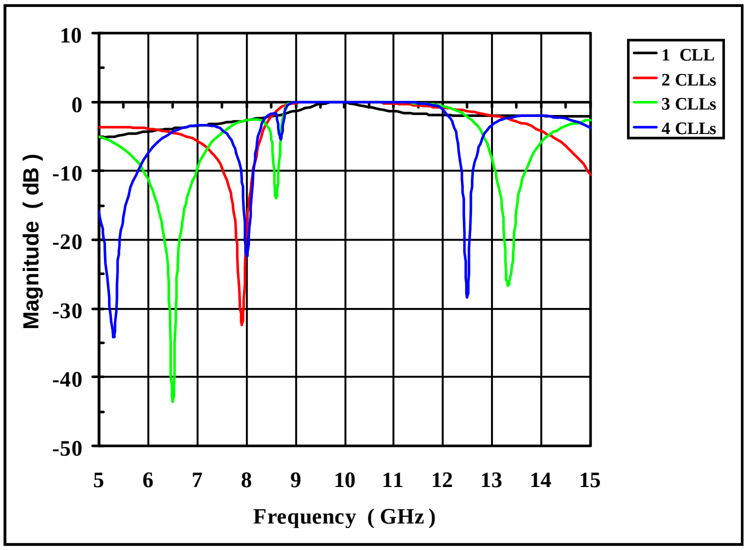

HFSS calculated S_{11} values for the CLL MTM with a depth of 4 CLL elements show that it acts as a PMC near the design frequency of 10GHz

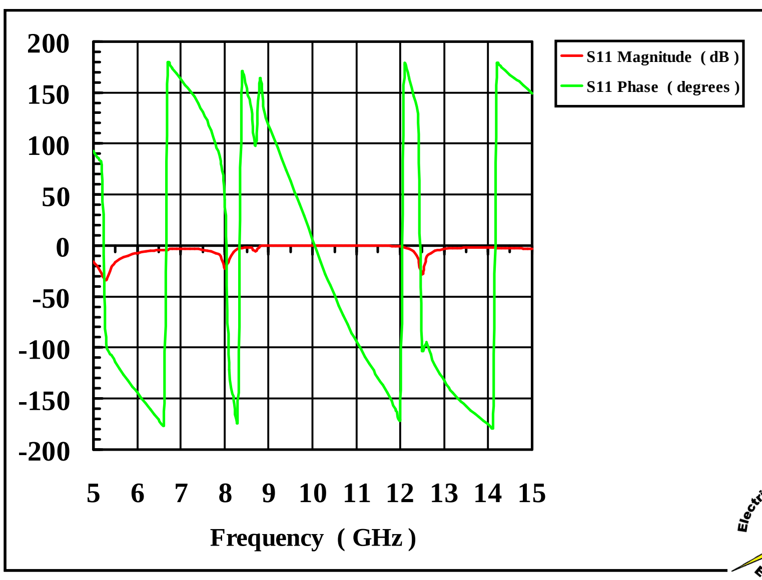

HFSS calculated S_{11} values for the CLL MTM with a depth of 4 CLL elements show that it acts as a PMC near the design frequency of 10GHz

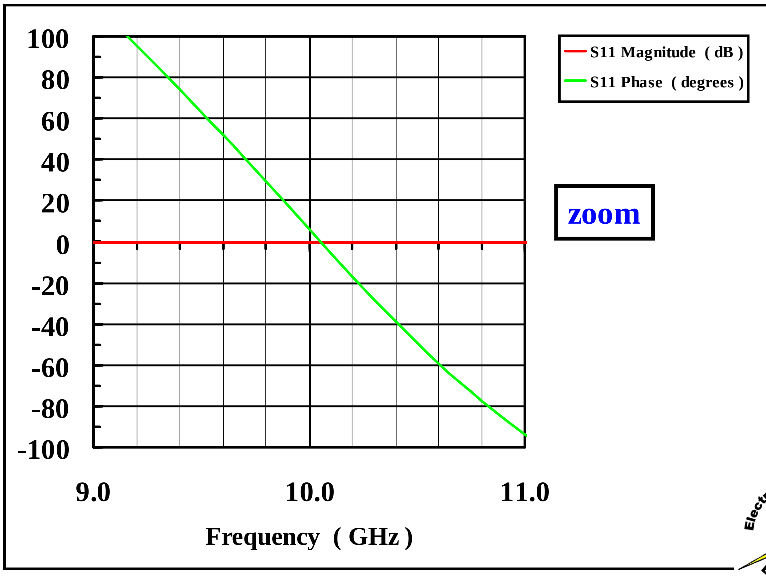

“Final” CLL Metamaterial Structure

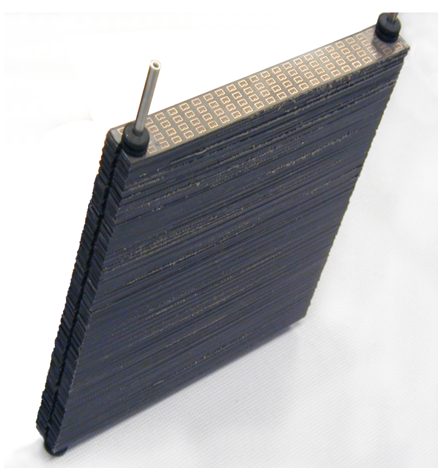

- “Precisely cut, aligned” and assembled of 161 strips

The CLL MTM was measured with a free space measurement system

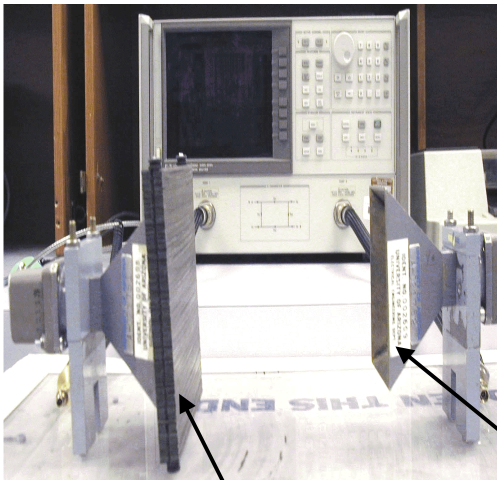

- **Measure the CLL MTM with its designed orientation**
- **Measure the CLL MTM with a 90° rotation**
- **HP 8720C network analyzer to measure the S-parameters**

Measured magnitude of S_{21} for the CLL MTM slab

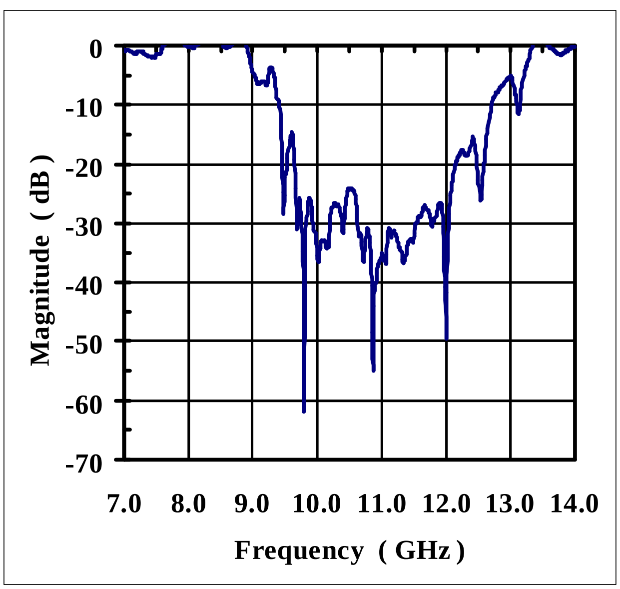

Measured magnitude of S_{11} for the CLL MTM slab

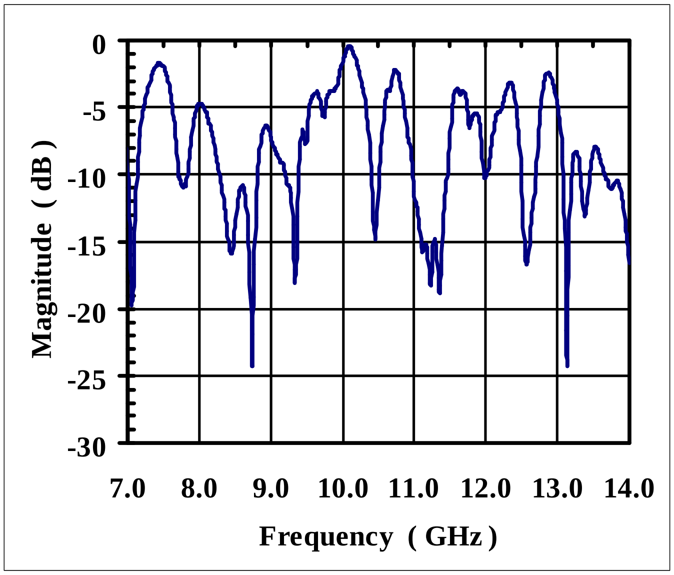

Phase Reference Plane measurement was achieved with a reference copper plate

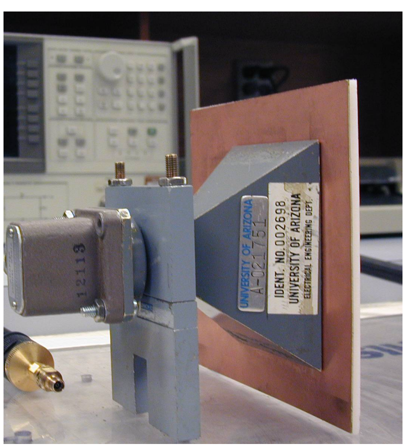

- A copper plate is placed over the mouth of the flange of the transmit antenna

Measured phase of S_{11} for the CLL MTM slab and for the reference plate

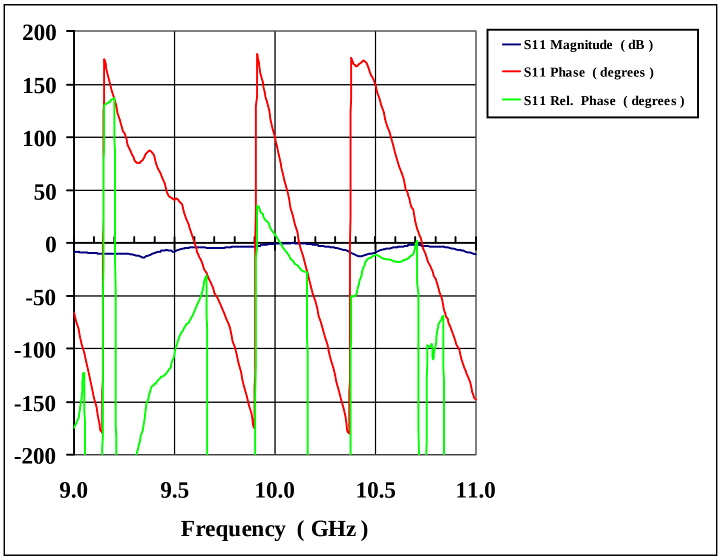

Measured magnitude and phase of S_{11} for the CLL MTM slab verifies the predicted PMC behavior

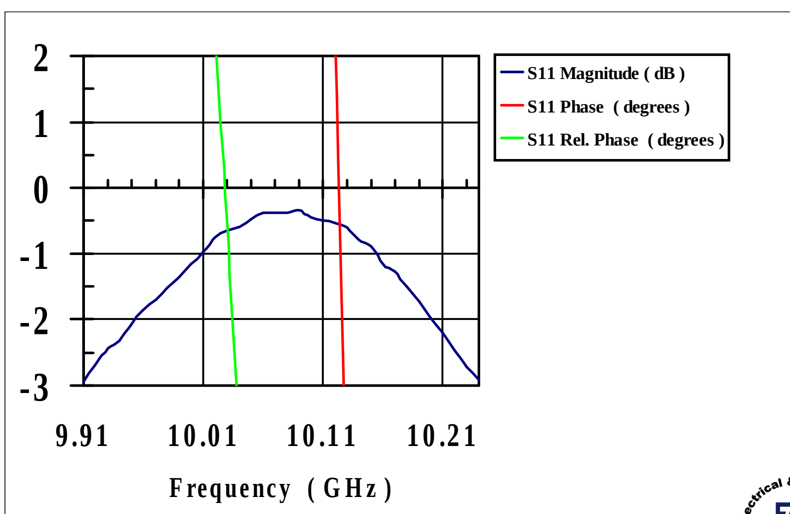

Measured magnitude of S_{11} for the CLL MTM slab in 90^{o} fixed rotatation demonstrates the expected anisotropy

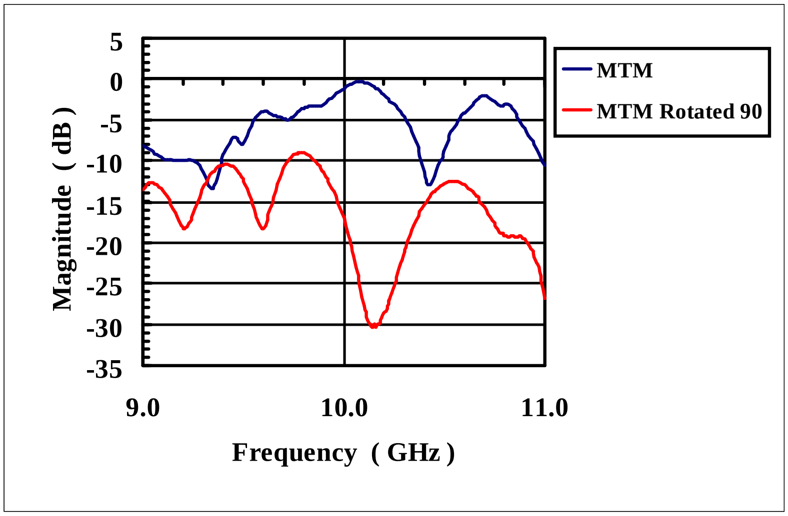

The relationships representing the power radiated by and the antenna Q of an electrically small antennas are well-known

Complex power for a small dipole in free space:

$$P = \int_0^{2\pi}\int_0^{\pi} \frac{1}{2} E_\theta H_\phi^* \, r^2 \sin\theta \, d\theta \, d\phi = \eta \frac{\pi}{3} \left| \frac{I_0 l}{\lambda} \right|^2 \left[1 - \frac{j}{(kr)^3} \right]$$

Changes sign for DNG medium

Antenna Q:

$$Q = \frac{1 + 2(ka)^2}{(ka)^3 [1 + (ka)^2]} \approx \frac{1}{(ka)^3} \qquad \textbf{for} \qquad ka << 1$$

Can a DNG spherical shell be used to improve the power radiated by an electrically small antenna??

We have solved analytically the problem of an electrically small linear dipole antenna surrounded by a spherical shell of DNG material

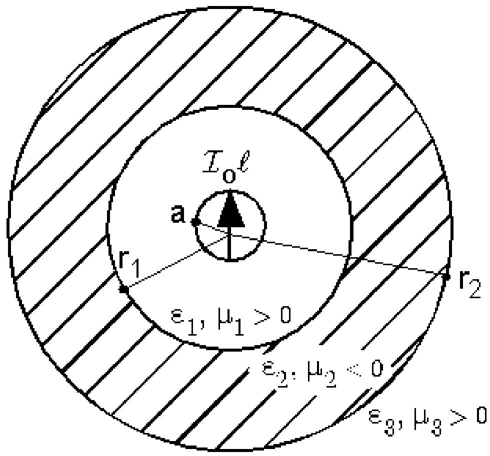

Allison Kipple, PhD candidate

Calculating the radiated power normalized to the small dipole value as a function of the radius r_2, we find that there several regions of where the radiated power is enhanced significantly and, correspondingly, where Q is reduced

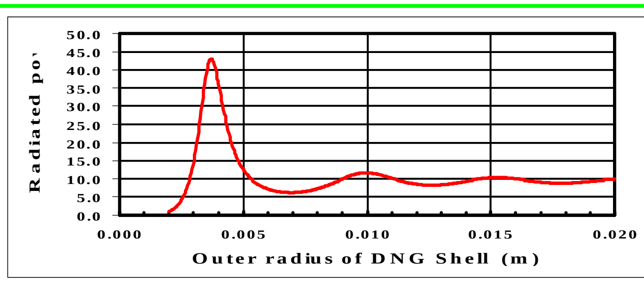

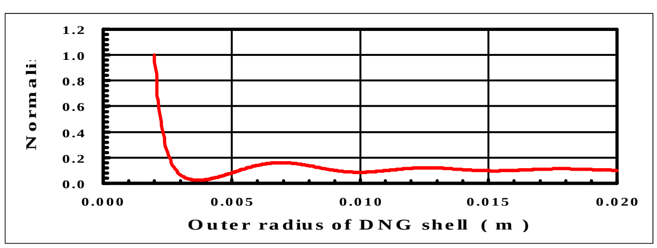

$a = \lambda / 750 = 4.0E\text{-}5$ m, $r_1 = \lambda/15 = 0.002$ m for $f_0 = 10$ GHz and $n = -3$

A very large power gain is predicted for a thin DNG shell AND with a reasonable bandwidth

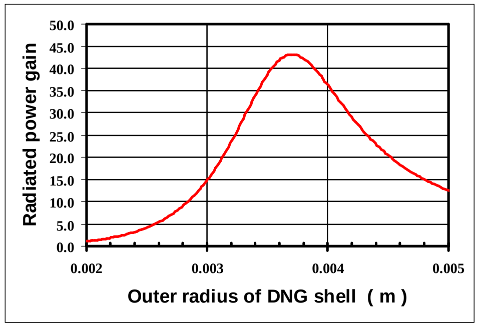

Antenna Q (normalized to free space value) is reduced to near zero where the large power gain occurs

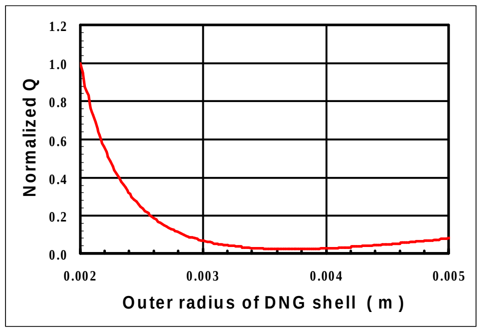

a = λ / 750 = 4.0E-5 m, r_1= λ/15 = 0.002 m for f_0 = 10 GHz and n = -3

Significant power gain with a reasonable bandwidth is predicted for a larger and thicker DNG shell

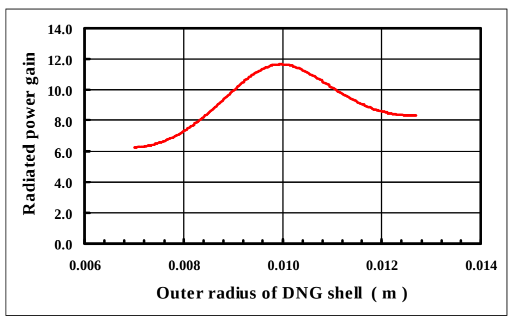

Antenna Q (normalized to Free space value) is reduced to near zero where the large power gain occurs

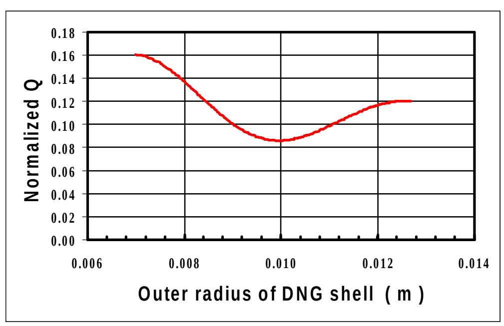

a = λ / 750 = 4.0E-5 m, r_1= λ/15 = 0.002 m for f_0 = 10 GHz and n = -3

Significant power gain with a reasonable bandwidth is predicted for a thin DNG shell that is closer to the dipole antenna

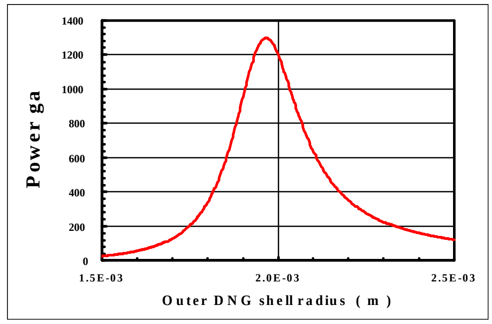

Antenna Q (normalized to Free space value) is reduced to near zero where the large power gain occurs

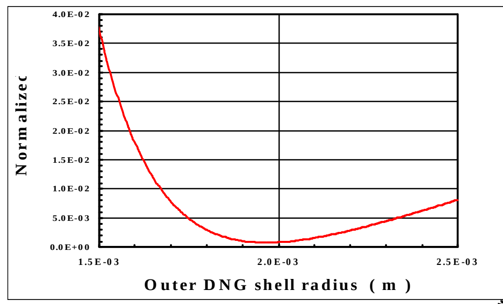

$a = \lambda / 1500 = 2.0E-05$ m , $r_1 = \lambda/30 = 0.001$ m for $f_0 = 10$ GHz and $n = -3$

An extremely large power gain is predicted for a very close proximity, thin DNG shell, BUT with an extremely narrow bandwidth

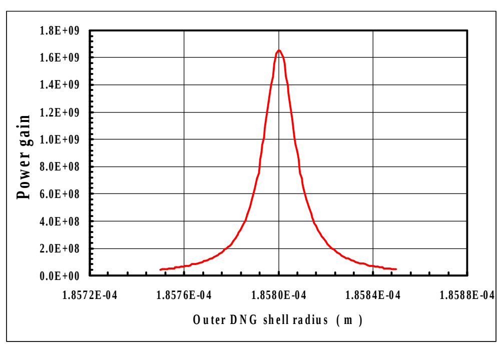

Antenna Q (normalized to free space value) is reduced to near zero where the large power gain occurs

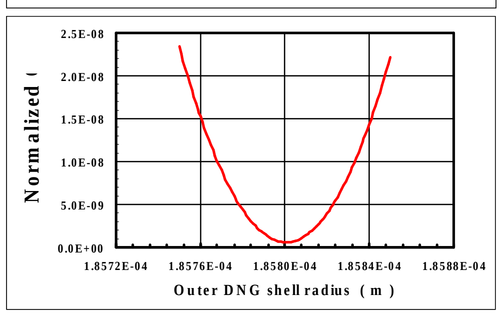

$a = \lambda / 15000$, $r_1 = \lambda/300 = 0.0001$ m for $f_0 = 10$ GHz and $n = -3$

Compact metamaterials having negative index of refraction have been designed, fabricated and tested experimentally

- **HFSS and FDTD simulators have been used to design several DNG ($\varepsilon < 0$ and $\mu < 0$) metamaterials (MTMs)**
- **Extraction formula have been derived to determine the MTM's effective permittivity and permeability**
- **Experimental results confirm the realization of DNG MTMs that are matched to free space and have a negative index of refraction**
- **Several potential applications have been studied: Efficient Electrically Small Antennas (EESAs)**

Thank you for listening ☺

Special Issue of IEEE Antennas and Propagation on Metamaterials

R. W. Ziolkowski and N. Engheta, Guest Editors

Contributions due October 1, 2002